COMPARING JUVENILE PHYSIOLOGY AND MORPHOLOGY OF TWO HIGH-ELEVATION PINES, *PINUS ALBICAULIS* AND *PINUS BALFOURIANA*

by

Katherine Elizabeth Sparks

A thesis submitted in partial fulfillment
of the requirements for the degree

of

Master of Science

in

Biological Sciences

MONTANA STATE UNIVERSITY
Bozeman, Montana

December 2023

DEDICATION

In dedication to my brother, Timothy Sparks. I know you would have done it better.

ACKNOWLEDGEMENTS

Thanks to Danielle Ulrich, Justin Runyon, Brian Smithers, and Katharine Banner for serving as my committee and helping me get over all the obstacles along the way to completing this project. Thanks to the US Forest Service Dorena Genetics Lab and Coeur d'Alene Nursery for donating plant material. Thanks to Ian Laga for helping me navigate the complexity of multivariate statistics and experimental design. Thanks to Maria Jerome for lending your experience and knowledge in troubleshooting all the xylem processing and for your encouragement along the way. Thanks to my fellow Ulrich lab members, Sean Hoy-Skubik, Franklin Alongi, Jessica Harris, Teodora Rautu, Lou Duloisy, Steve Huysman, and Chloe Wasteneys for all your input, assistance, and friendship along the way. Thanks to Ethan Fuchs, Bobby Beers, Tristan Burlingame, Timothy Jones, Grace Miller, Naomi Vliet, Benjamin Spiers, William Lutz, Gabrielle Ostrowski, David Heinson, David Rossal and all the other undergraduate students who helped along the way – I never would have finished this thesis without you guys! Thanks to Shreya Gautam, Anna French, Thomas Meinzen, Molly Burchfield, Kelsey Flathers, Terry Hamburg, Robert Eckelbecker, Mary Greene, Nate Heili, Jacob Crooks, Addison Marcus, Jennifer Hardy, Jordan Rainey, Dipiza Oli, Matthew Nunnery, and Hannah Goemann for getting me through grad school. And finally, thanks to my family for being there for me through the good and bad times.

TABLE OF CONTENTS

TABLE OF CONTENTS CONTINUED

LIST OF TABLES

Table Page

LIST OF FIGURES

Figure Page

LIST OF FIGURES CONTINUED

Figure Page

LIST OF FIGURES CONTINUED

Figure Page

ABSTRACT

Whitebark pine (*Pinus albicaulis*, PIAL) and foxtail pine (*P. balfouriana*, PIBA) are slow-growing, high-elevation, five needled ("high five") white pines and are foundation and keystone species in alpine and subalpine environments, providing essential resources and habitat for many species including the Clark's nutcracker and grizzly bears. In recent years, PIAL has experienced significant decline due to an amalgamation of climate change, white pine blister rust, and mountain pine beetle. As a result, PIAL is listed as endangered under the Canadian Species at Risk Act and threatened under the United States Endangered Species Act. Conversely, PIBA has experienced minimal decline. PIBA also exists in two disjunct populations, one in southern California ($PIBA_S$) and one in northern California ($PIBA_N$), resulting in the species being split into two sub-species (*P. balfouriana* subsp. *austrina* and *balfouriana*). Our study compared the physiology and morphology of the two species (PIAL and PIBA) and the two foxtail populations ($PIBA_N$ and $PIBA_S$) to better understand how they interact with and respond to abiotic and biotic stressors in their high-elevation environments. We grew four-year-old PIAL and PIBA juveniles in a common greenhouse environment. In total, we measured 159 traits describing their morphology, biomass, stomata, xylem, budburst phenology, physiology, whole plant Volatile Organic Compounds (wpVOCs), phloem volatile resin (PVR) compounds, and Non-Structural Carbohydrates (NSCs). We found that PIAL and PIBA displayed different suites of traits that enable them to persist in their high elevation habitats, characterized by similar abiotic stressors (cold temperatures, high winds, summer drought) and biotic stressors (white pine blister rust, bark beetle). The two foxtail populations were similar for most traits except for wpVOC concentration and composition where $PIBA_S$ had significantly higher wpVOC concentration than $PIBA_N$. For most traits, PIAL was most similar to $PIBA_N$ and differed the most with $PIBA_S$ while $PIBA_N$ was the intermediate being more similar to both groups, especially in wpVOC composition and concentration.

INTRODUCTION

High elevation, five-needled pines (commonly referred to as "high-five pines") are keystone and foundation species with distributions spanning North America from southern California into Northern Canada (Gibson et al., 2008). High-five pines are often the only tree species that can establish in subalpine ecosystems, meaning they define both the function and aesthetics of these habitats (Campbell et al., 2011). North American high-five pines are a closely-related group of white pines consisting of six species: whitebark pine (*Pinus albicaulis*), southwestern white pine (*P. strobiformis*), limber pine (*P. flexilis*), Great Basin bristlecone pine (*P. longaeva*), Rocky Mountain bristlecone pine (*P. aristata*), and foxtail pine *(P. balfouriana*) (Tomback & Achuff, 2010).

As keystone and foundation species, high-five pines provide numerous services to their ecosystems. They play a major role in the hydrologic cycle by stabilizing snowpack and regulating downstream flow by decreasing the rate of snowmelt (Farnes, 1989). High-five pines also play an important role in seral succession for alpine and subalpine ecosystems. These systems are characterized by high winds, unpredictable precipitation patterns, cold temperatures, snow, and intense solar radiation – conditions which make it uninhabitable for most other species (Campbell et al., 2011). High-five pines have developed a slow-growing life strategy which allows them to establish in these harsh conditions, and in turn creates a more suitable habitat for other species to establish and survive (Baumeister & Callaway, 2006). High-five pines also are important to the food webs of alpine and subalpine ecosystems. Because of their high percentages of essential fats and amino acids, whitebark pine and limber pine seeds in particular are a main food source for numerous species, including grizzly bears and Clark's Nutcrackers

(Felicetti et al., 2003; Schaming & Sutherland, 2020). Through their regulation of habitat and food resources, these trees play a vital role in the function and persistence of alpine and subalpine ecosystems.

High-five pines, especially whitebark pine, have recently been experiencing an alarming rate of mortality and decline, a primary concern for managers due to these pines' invaluable ecosystem services (Hankin & Bisbing, 2021). Across the western US, the percentage of dead trees was approximately 42% for limber pine and 54% for whitebark pine as of 2020 (Goeking & Windmuller-Campione, 2021). Foxtail pine, Rocky Mountain bristlecone pine, Great Basin bristlecone pine, and southwestern white pine all averaged about 18% dead of total observed trees, suggesting that these species are less affected or respond differently to stress than limber or whitebark pine (Tomback et al., 2022). This widespread forest mortality has the potential to fundamentally alter the abundance and distribution of high-five pines. Therefore, we need to understand the causes of these population declines and the physiological mechanisms of individual tree mortality in order to predict the future of these ecosystems.

Both abiotic and biotic stressors play a role in the decline of the high-five pines. Global temperatures have increased by 1.5°C since 1900, causing fundamental changes in many ecosystems worldwide (IPCC, 2018). Increasing temperatures induce heat stress in high-five pines, which is a factor that can cause mortality on its own. However, increases in temperature also lead to decreases in snowfall, which makes up the largest percentage of precipitation for these ecosystems (Badger et al., 2021). Decreasing snowfall leads to reduced snowpack and increased drought conditions which can contribute to additional mortality (Keane et al., 2017). Alpine and subalpine ecosystems are particularly vulnerable to climate change because of their

high sensitivity to long-term change of temperature and precipitation patterns (Kueppers et al., 2017). Researchers predict the rate of temperature increase will be higher in subalpine regions, giving species less time to adapt to the change (Adhikari et al., 2018). In addition, while most other species can migrate to higher elevations as global temperatures rise, subalpine species often already exist on or near mountaintops and are thus unable to migrate upwards. Because high-elevation five-needle pines have adapted to harsh subalpine ecosystems with reduced competition among plants for resources, they are likely less able to compete with encroaching species that are adapted to the warmer climate (Perez-Garcia et al., 2013). Finally, high-five pines have low growth rates, long generation times, dispersal limitations, delayed seed germination, and high mortality rates, which can result in mortality outpacing regeneration (Dullinger et al., 2004a; Tomback et al., 2001).Increased heat and drought conditions cause high-five pines to become more susceptible to biotic stressors (Erbilgin et al., 2021; Shanahan et al., 2016). Currently, there are three main biotic factors threatening high-five pines: white pine blister rust (*Cronartium ribicola*), mountain pine beetle (*Dendroctonus ponderasae*), and dwarf mistletoe (*Arceuthobium* spp.) (Shanahan et al., 2019). White pine blister rust, a non-native fungal pathogen, is currently the leading cause of mortality in whitebark pine and is steadily expanding in range to affect an increasing percentage of all high-five pines (Schoettle, 2004). Though some species are more rust-resistant than others (Dudney et al., 2020; Sniezko & Liu, 2022) and blister rust has not yet been observed in all high-five pine species habitats (Nesmith et al., 2019; Schoettle et al., 2022a), it is important to understand the impacts and future ramifications for all species affected by this invasive pathogen. Since the recent introduction of white pine blister rust around 1900, several high-five pines have experienced devastating mortality rates, especially whitebark pine (Thoma et al., 2019). Increasing temperatures and higher humidity create more

suitable growing environments for white pine blister rust while correspondingly reducing the ability of trees to defend against the pathogen (Thoma et al., 2019; Young et al., 2023). As temperatures continue to increase, previous research predicts the severity of white pine blister rust will correspondingly increase (Wyka et al., 2018).

Both dwarf mistletoe and mountain pine beetle are endemic to the range of high-five pines and therefore have antagonistically co-evolved pathogen-host interaction strategies allowing them to sustainably co-exist until recently (Morgan & Koskella, 2011; Shanahan et al., 2019). Heat and drought stress have reduced the capacity of high-five pines to defend against mountain pine beetle and parasitic mistletoe (Erbilgin et al., 2021). Much like white pine blister rust, warmer climates are more favorable to mountain pine beetle and mistletoe. Shorter, warmer winters and longer growing seasons advance and expand the bark beetle life cycle, increasing total beetle populations and expanding their range (Bentz et al., 2016a, 2022; Runyon et al., 2022a; Soderberg et al., 2022). For these reasons, an upward trend in mortality from mountain pine beetle and mistletoe is predicted to be observed with increasing temperatures and increasing drought events (Keen et al., 2022).

Current high-five pine research focuses predominantly on adult tree mortality, with relatively little research investigating the seedling and juvenile stages. Both the ability for seedlings to establish as well as the ability of juveniles to survive are necessary for the species to remain extant in their current climates and geographic distributions. In addition to adult mortality, the success, growth, and survival of young developmental stages (such as seedling and juvenile stages) can alter species distributions (Hansen et al., 2021). Therefore, to better predict future species distributions, we need to understand the physiological mechanisms or traits

underlying juvenile growth and survival under their range's current and future climates. The physiological traits that determine juvenile growth and survival include traits that affect the ability to obtain CO_2, water, and light, as well as traits that affect the ability to resist or tolerate both abiotic and biotic stress. Examples of such physiological traits are photosynthetic performance, stomatal traits (such as conductance, density, and size), xylem characteristics (such as tracheid density and size, potential hydraulic conductivity), non-structural carbohydrate (NSC) concentrations in needles, stems, and roots, and volatile organic compound (VOC) concentration and composition. Each of these physiological traits contributes to how a plant obtains and uses the "ingredients" for photosynthesis, allocates the products of photosynthesis, and/or withstands environmental stress. Such physiological traits determine the growth and survival of a juvenile and therefore also the climates in which it can persist and a species' geographic distribution.

For instance, traits describing stomatal size and density can give us insight into how a plant is taking up CO_2 and losing water through its stomata (Holland & Richardson, 2009). As another example, NSCs (including starch, sucrose, glucose, and fructose) are products of photosynthesis that influence the ability of a plant to cope with drought. NSCs can act as both solutes for osmoregulation and as emergency carbon reserves in times of drought stress when the plant closes its stomata for water conservation and therefore cannot take up CO_2 (Hartmann & Trumbore, 2016). Therefore, understanding what NSCs are present, in what concentration, and in what tissue (needles, stems, roots) can reveal how juveniles allocate carbon when under stress (Huang et al., 2017). As a final example, plant secondary chemistry (like toxic compounds within-phloem and VOCs emitted from plants) can also act as a tool of defense against abiotic stressors through mechanisms like thermoregulation and cell stabilization, as well as defense

against biotic stressors by acting as repellents or toxins (Rissanen et al., 2022). Just like with NSCs, secondary chemistry is part of a plant's carbon pool, is important for carbon allocation under stress (Kreuzwieser et al., 2021). Examining all of these physiological traits together can create an overarching picture of how high-five pine juveniles physiologically respond to current and future environmental stress.

Common garden or common environment experiments are powerful tools for comparing physiological and morphological traits between species and populations and enabling us to identify whether traits are expressed as a result of phenotypic plasticity and/or genetic variation. Individuals of different species and/or populations are planted in a common controlled environment, which eliminates confounding factors that can influence plant traits such as climate, species competition, and anthropogenic disturbance (de Villemereuil et al., 2016). In doing so, common environment experiments allow us to determine whether the expression of a trait is driven primarily by: phenotypic plasticity (relatively shorter term adjustments in response to the plant's current environment), or genetic adaptation (relatively longer term heritable traits that reflect the individual's genetics, population, and/or species) (McLane & Aitken, 2012). Because all other variables are being held constant in common environment experiments, trait differences observed between species or populations suggest that that trait's expression is driven by genetics, while in contrast, trait similarities observed between species or populations suggest that the trait's expression is driven by phenotypic plasticity, reflecting the common environment under which both species or populations are growing (Schwinning et al., 2022). Understanding drivers of physiological trait expression are important for understanding species' response to

future climate, which allows us to better predict future species distribution, improving management plans for these species.

Despite their many similarities, species within the high-five pine group may respond differently to abiotic and biotic stressors, causing variable and species-specific levels of mortality and distribution shifts, and suggesting that they have adapted different strategies and physiological mechanisms to persist in their high-elevation environments (Goeking & Windmuller-Campione, 2021). In order to better predict how these species will be impacted by future climates, we need to understand their physiological and morphological traits and responses to stress. Currently, the high-five species of most concern is whitebark pine (*P. albicaulis*; PIAL), as it has experienced the highest rates of mortality in western North America (Goeking & Windmuller-Campione, 2021). PIAL is native to North America with the broadest and most northerly distribution of all high-five pines, spanning from southern California into northern Canada (Figure 1). PIAL has been listed as endangered under the Canadian Species at Risk Act since 2012 and was recently listed as threatened under the United States Endangered Species Act of 1973 in 2021 (Government of Canada, 2017; USFWS, 2022). While multiple stressors have played a role in the decline of PIAL, white pine blister rust is the leading cause of mortality (Landguth et al., 2017). As a result, current management practices consist of outplanting rust-resistant seedlings to mitigate population loss through replacement of dead trees with seedlings and juvenile trees (Fiedler & McKinney, 2014). However, the incredibly slow growth rate of PIAL leads to minimal recruitment and a decades-long delay between planting and stand regeneration, creating a race between mortality rate and stand regeneration (Dullinger et al., 2004b; Tomback et al., 2001, 2022). Additionally, rust resistance is currently the only trait

being selected for across PIAL seed sources, while tolerance to other stressors is being overlooked (Keane et al., 2017). A possible reason for this oversight is the current lack of knowledge of the effects other stressors have on seedling and juvenile growth and survival (Dudney et al., 2020). Water availability and temperature are main factors in determining seedling and juvenile success, making it important to examine physiological and morphological traits that affect their ability to survive abiotic and biotic stress (Johnson et al., 2011). This knowledge will inform management decisions on seed source selection for outplanting and optimize this restoration method.

In contrast to PIAL, the mortality rate of foxtail pine (*P. balfouriana*; PIBA) is approximately 17%, causing PIBA to currently be listed as "near-threatened" by the International Union for Conservation of Nature (IUCN, 2011). PIBA is located only within the state of California and can be found between 1500 to 3500 m elevations while PIAL's distribution spreads latitudinally all the way into northern Canada in elevations between 900 to 3660 m (Figure 1; Campbell et al., 2011). Although they exist in similar elevation ranges, because of their differences in latitudinal ranges, PIBA populations typically have warmer growing season temperatures and higher levels of winter precipitation than PIAL (Campbell et al., 2011; Goeking & Windmuller-Campione, 2021; PRISM Climate Group at Oregon State University, 2020). In recent surveys of PIBA's distribution, there has been no evidence of infection from white pine blister rust and minimal mountain pine beetle-induced mortality, possibly due to minimal exposure to white pine blister rust and stronger defense against mountain pine beetle (Bentz et al., 2016a; Dudney et al., 2020; Nesmith et al., 2019; Schoettle et al., 2022a). However, increases in temperature and drought will both expand the range of white pine blister rust to

overlap with PIBA's distribution (Landguth et al., 2017). Not only will increased temperature and drought stress render PIBA less able to defend against both white pine blister rust and mountain pine beetle, recent studies have also found that PIBA has the lowest level of resistance to white pine blister rust of all high-five pines (Sniezko & Liu, 2022). In contrast, PIBA has unique VOC compositions which increase its defensive capabilities against mountain pine beetle (Bentz et al., 2016a; Dudney et al., 2020; Nesmith et al., 2019; Schoettle et al., 2022a). Currently, occurrences of white pine blister rust are minimal in PIBA's species range, but it is unclear how this will change under future climates (Dudney et al., 2020; Schoettle et al., 2022a; Sniezko & Liu, 2022; Wyka et al., 2018). If beetle and/or rust-induced PIBA mortality rates do increase, managers may apply lessons learned from the PIAL outplanting conservation strategy to PIBA. However, we lack a direct comparison of PIAL and PIBA's seedling and juvenile physiological mechanisms to survive stress.

In contrast to the relatively unfragmented distribution of PIAL that allows for gene flow between populations, PIBA has a uniquely disjunct distribution split between two geographically isolated populations. PIBA is endemic only to California and its distribution is divided by over 500 km into a southern population in the Sierra Nevada and a northern population in the Klamath mountains (Eckert et al., 2008). Because of the complete separation between southern and northern populations, the lack of gene flow between the two populations has created conditions for divergent evolution and speciation (Oline et al., 2000). For this reason, the species is split into two sub-species – *P. balfouriana* subsp. *balfouriana* (northern foxtail pine; $PIBA_N$) and *P. balfouriana* subsp. *austrina* (southern foxtail pine; $PIBA_S$) (Bentz et al., 2016b). Like PIAL, $PIBA_N$ and $PIBA_S$ exist in high-elevations with nutrient-poor soils, high windspeeds, periods of

drought during growing seasons, and high-light exposure (Campbell et al., 2011). However, $PIBA_N$ exists at lower elevations than $PIBA_S$, and therefore can be characterized by warmer temperatures and higher winter precipitation than $PIBA_S$ (Campbell et al., 2011; Goeking & Windmuller-Campione, 2021; PRISM Climate Group at Oregon State University, 2020). Currently, very little is known about the seedling and juvenile stages of PIBA for either population (Fryer, 2004). A physiological and morphological comparison of the two PIBA populations will increase our understanding of how the overall species distribution may be affected under future climate conditions.

For our study, we investigated four research questions: (1) Are there measurable physiological trait differences between PIAL and PIBA juveniles? (2) Are there measurable physiological trait differences between PIAL, $PIBA_N$, and $PIBA_S$ juveniles? (3) Are there measurable physiological trait differences between $PIBA_N$ and $PIBA_S$? (4) How does drought stress affect the physiology of PIAL, $PIBA_N$, and $PIBA_S$ juveniles? We hypothesize that climate of origin will drive differences in physiological traits for all comparisons. More specifically, we hypothesize that: (1) PIAL will exhibit more stress tolerant traits than PIBA, allowing PIAL to persist in colder, drier climates than PIBA, (2) PIAL will share more similarities with $PIBA_S$ than with $PIBA_N$ because $PIBA_S$ has colder, drier climates than $PIBA_N$, (3) $PIBA_S$ will exhibit more drought resistant traits than $PIBA_N$ because $PIBA_S$ persists in drier climates than $PIBA_N$, and (4) PIAL will resist drought stress more so than PIBA because PIAL persists in drier climates than PIBA. To test these hypotheses, we conducted a common environment greenhouse experiment exposing PIBA and PIAL juveniles to drought and control treatments and measuring

a suite of physiological and morphological traits before, during, and after treatment to compare the physiology, morphology, and drought stress response between PIAL, $PIBA_N$, and $PIBA_S$.

METHODS

Study Material

Sixty-two four-year-old (juvenile) whitebark pine individuals (*Pinus albicaulis,* PIAL) were donated by the Coeur d'Alene US Forest Service Nursery (Coeur d'Alene, ID, USA), and 14 four-year-old foxtail pine individuals (*Pinus balfouriana,* PIBA) were donated by the Dorena Genetic Resource Center US Forest Service Nursery (Cottage Grove, OR, USA). Thirty of the PIAL juveniles were grown from seeds collected from three sites (1 family per site) in Idaho (Burke) and Montana (Big Mountain, Jefferson) (Figure 1). A family refers to juveniles grown from seeds of the same parent tree. The remaining 32 PIAL juveniles were grown from seeds collected from sites in Idaho (Burke), Wyoming (JHMR), and Montana (7694, 7678, Big Mountain, Wheeler Mountain), though their identification tags were lost so each of the 32 individuals' specific family is unknown (Appx. Table 1). We included these 32 PIAL in our study to increase our sample size because they originated from our families of interest and our previous unpublished work has not revealed significant physiological differences between these PIAL families. We grouped our PIAL juveniles into three groups: Burke/Big Mountain ($PIAL_{BBM}$, because there were negligible differences between these two family seed source climates), Jefferson ($PIAL_{Jeff}$), and unknown ($PIAL_{Unk}$). PIBA juveniles were grown from seeds collected from two sites (1 family per site; family names: '267' and '330') in the northern population ($PIBA_N$) and two families (1 family per site; family names: '296' and '314') from the southern population ($PIBA_S$). A population refers to a group of families within the same geographic area and gene pool (Figure 1, Table 1). All juveniles had a year-long acclimation period from June 2021 to June 2022. We transplanted PIAL and PIBA juveniles on 17 January

2022 and 8 April 2022, respectively, into tree pots (19 cm x 19 cm x 46 cm) with a peat-perlite soil medium (Sunshine #1 mix – Sungro, Agawam, MA, USA). Our measurement period began in June 2022 and ended in December 2022.

All juveniles were grown in the Plant Growth Center (Montana State University, Bozeman, MT, USA). Supplemental lighting was provided to maintain a minimum 16-hour photoperiod during the one-year acclimation period. During the measurement period, no supplemental light was provided, average photosynthetically active radiation (PAR) was 145.4873 W/m^2, temperatures averaged 20.7°C during the day and 16.4°C during the night, with a maximum temperature of 31.3°C and a minimum temperature of 8.7°C, and average relative humidity was 55.84%, with a high of 95.2% and a low of 13.4%.

Experimental Design

Treatments began on 12 June 2022 and ended on 9 December 2022. In the drought treatment, target volumetric water content (VWC) was 5% based on previous measurements to create moderate drought conditions using a method adapted from (Marchin et al., 2020) as follows. Tree pots were firmly placed atop floral foam blocks (Oasis IDEAL Floral Foam Maxlife brick; Smithers-Oasis, Kent, OH, USA) that sat in large, plastic bins (27 gal/102.2 L heavy duty totes; Project Source). We drilled nine 2-cm diameter holes in the bottom of each tree pot to provide connection between soil and floral foam. Tree pots were firmly pressed down on top of foam blocks to ensure that floral foam came directly in contact with soil, with six pots in each bin. We controlled VWC for the drought and control treatments by varying the water level within each bin (Figure 2). We determined the water level needed for desired VWC in a

pilot study using 12 PIAL juveniles which were then removed from the experiment. The water level was set at 20 cm for control bins and 10 cm for drought bins. Treatment (drought, control) was randomly assigned to each bin. Then, juveniles were randomly distributed to each bin using an unbalanced incomplete block design with each family and species represented in each bin as equally as possible (because not all families had even numbers of individuals). We ensured that bins with $PIBA_N$ also had $PIBA_S$ and at least one PIAL group present. For bins that were not able to have $PIBA_N$ or $PIBA_S$ represented due to low numbers of trees, we prioritized equally representing the three PIAL groups ($PIAL_{BBM}$, $PIAL_{Jeff}$, $PIAL_{Unk}$). Each bin contained between 4 and 6 individuals for this study. For bins that filled only 4 of the 6 positions, the remaining positions were filled with individuals for a separate study (Appx. Figure 2).

Treatments lasted 24 weeks (15 June 2022 to 28 November 2022) with the goal of creating a significant and biologically meaningful difference in predawn leaf water potential between drought and control treatments, which we defined as a difference of greater than 1.0 mPa between treatment and control. Predawn and midday leaf water potentials and VWC were measured weekly throughout the 24 weeks using a handheld VWC sensor (Hydrosense II, Campbell Scientific, Logan, UT, USA). Additionally, continuous hourly VWC was tracked using digital sensors (SDI-12; Meter Environment, Pullman, WA, USA) placed directly in the soil for one juvenile per bin and divided so PIAL, $PIBA_N$, and $PIBA_S$ had at least one sensor in both drought and control (due to minimal resources only eight pots had continuous VWC sensors). Because VWC did not reach below the desired 5% in the drought treatment and VWC was above desired levels for control treatment, we decreased water levels by 10 cm for both treatments during weeks 11-24 of the experiment. Following the experiment, between 28 November 2022

and 9 December 2022, we destructively harvested all juveniles in a stratified randomized order designed to equally distribute species and families (PIAL, $PIBA_N$, $PIBA_S$) across harvest days, for measurements described below.

Morphology and Biomass

Following the destructive harvest of all juveniles, morphological and biomass trait measurements were made 10 March 2022 – 25 March 2022. We measured live stem base diameter, stem height, stem base diameter:stem height, fascicle density (FD), branch diameter, branch length, branch diameter:branch length, leaf mass per area (LMA), sapwood area:leaf area (SA:LA), and the ratio of sunlit leaf area to total leaf area (STAR). In addition, we measured dried biomass (needle, stem, root, aboveground:belowground). We measured stem base diameter and terminal stem height using calipers, from which we calculated stem diameter:height. For branch diameter, branch length, branch diameter:branch length, and FD, we selected three first order lateral branches and measured their diameter one centimeter from the main stem and their length from main stem to apical bud using calipers and counted the total number of fascicles on the branch. FD was calculated for each of the three branches as the total number of fascicles divided by total branch length. FD, branch diameter, branch length, and branch diameter:branch length were averaged across the three branches for each individual.

LMA was calculated for the largest first order lateral branch as the ratio of fresh leaf area to the total dry leaf biomass. Fresh leaf area was measured from an image of all needles from a single branch laid flat with no overlap using Fiji (previously ImageJ; Schindelin et al., 2012). We measured dry leaf biomass by placing all needles from the same single branch into a coin

envelope and drying for 72 h at 45 °C after harvesting and prior to weighing. SA:LA was calculated as the ratio of sapwood area (defined as functional conducting tissue) to fresh leaf area. Sapwood area was determined by cutting a 0.25-cm section from the base of the branch (the same branch used to measure fresh leaf area) to expose the cross section. We imaged the cross section and analyzed images using the freehand tool in Fiji measuring the cross-sectional area minus the bark area (Schindelin et al., 2012).

STAR was calculated as the ratio of the total sun-exposed leaf area to the total fresh leaf area for the whole individual. To measure total sun-exposed leaf area, we took top-down images of each individual on a neutral background using a Samsung Galaxy S20 FE phone camera. Total sun-exposed leaf area was measured using Trainable WEKA Segmentation (TWS), a plug-in available for Fiji. We used the TWS default classifier, FastRandomForest (Reutemann, 2022), and trained the classifier on 20 images (ten from each species) to identify and segment the individual from the neutral background. We ran all images through our trained classifier using the Fiji macros plug-in. The classifier created probability maps which we converted to binary 8-bit images prior to measuring area. Total fresh leaf area was calculated using the following equation:

$$A_T = m_T \cdot \frac{A_b}{m_b}, \quad (1)$$

where A_T is total fresh leaf area, m_T is total dry leaf mass, A_b is the previously measured fresh leaf area from the largest first order lateral branch, and m_b is the previously measured dry leaf biomass from the largest first order lateral branch. To determine biomass measurements (needle, stem, root, aboveground:belowground), we separated, dried, and weighed needles, stems, and

roots after harvesting. These samples were also analyzed for non-structural carbohydrates (see description below).

Stomatal Traits

Stomatal traits included aperture area, guard cell area, stomatal length, and stomatal density and were measured between 9 March 2022 and 23 March 2022. Five needles were taken from each of the three branches previously selected for FD measurements (described above). Fresh needles were stored in sealed Ziplock bags with moist paper towels in the dark between sampling and processing and were processed within five hours of collecting to ensure needles retained moisture. Fresh needle stomatal impressions were made by painting clear nail polish across the abaxial side of the needle. We allowed nail polish to thoroughly dry before firmly pressing clear cellophane tape onto the dried nail polish. The needle was then carefully peeled back from the tape, leaving only the nail polish impression of the stomata. We placed the tape onto a microscope slide, avoiding air bubbles, and viewed stomatal impressions under a light microscope (Micromaster, Fisher Scientific, Hampton, NH, USA) at 100x magnification. The highest quality portion of the impression was imaged using Swift Imaging 3.0 software with a SwiftCam SC500 (Swift Optical Instruments, Shertz, TX, USA). We measured aperture area using the freehand tool in Fiji, circling the inside opening of the stomata (not including guard cell area). We measured guard cell area by using the freehand tool in Fiji to circle the entire stomate (both aperture area and guard cell area) and calculated guard cell area by subtracting aperture area from the total stomatal area. Stomatal length was measured as the longest distance from one side of the aperture to the opposite side of the aperture using the line tool in Fiji. Stomatal density was measured as the number of stomata per row divided by row length.

Xylem Traits

After harvesting, a 1-cm fresh stem segment was cut from the base of each juvenile stem, dried for 72 h at 45 °C before being rehydrated and embedded in paraffin wax to stabilize cell structure for sectioning. Stem samples were sectioned transversely using a hand sliding rotary microtome (Leica Biosystems, Wetzlar, Germany) set at 16-µm thickness. Sections were fixed to slides and deparaffinized, then stained with toluidine blue for clear visualization. We imaged stained sections with a standard light microscope (Micromaster, Fisher Scientific, Hampton, NH, USA) at 100x and 1000x magnification using a microscope camera (Swiftcam SC1003-CK, Swift Optical Instruments, Shertz, TX, USA) and Swift Imaging 3.0 software. We stitched image tiles (100x magnification) together to create a complete stem cross section (Figure 3).

We measured annual earlywood (EW) ring width, annual latewood (LW) ring width, annual total ring width, resin duct area and density, EW and LW tracheid area, EW and LW tracheid density, EW and LW cell wall thickness, potential hydraulic conductivity (K_p), and vessel implosion resistance (VIR, a proxy for structural integrity). We measured EW ring width and LW ring width at four randomly selected locations per growth ring and averaged them to obtain a single EW, LW, and annual (EW + LW) width per ring per individual. We calculated annual ring width by adding EW and LW averaged widths for each ring and EW:LW ratio by dividing EW ring width by LW ring width. For resin duct area,we measured the area of all resin ducts within a stem cross section and calculated mean resin duct area. Resin duct density was calculated as the total number of resin ducts divided by total mm^2 of the stem cross section. For EW and LW tracheid area and cell wall thickness, we measured all cells in three randomly selected EW and LW $9.97x10^{-3}$ mm^2 sections per growth ring at 1000x magnification for a total

of six measured sections per growth ring. To measure tracheid area, we used the freehand tool in Fiji to circle all tracheids in each imaged section for all six 1000x sections. To measure tracheid cell wall thickness, using the line tool in Fiji, we measured 25 total double cell walls (Figure 4) per imaged section and divided each double cell wall thickness by two to achieve 50 total single cell wall measurements per imaged section.

Potential hydraulic conductivity (K_p) was calculated using the Hagen-Poiseuille equation for EW and LW separately (K_{pEW}, K_{pLW}). We calculated K_p as(Sterck et al., 2008):

$$K_p = K_{pEW} + K_{pLW}, \tag{2}$$

where K_{pEW} and K_{pLW} are calculated using the following equations (S. Yang et al., 2022):

$$K_{pEW} = \frac{\pi \rho_w}{128\eta} \times CD_{EW} \times D_{EW}^4, \tag{3}$$

$$K_{pLW} = \frac{\pi \rho_w}{128\eta} \times CD_{LW} \times D_{LW}^4, \tag{4}$$

where ρ_w is the density of water (998.2 kg m^{-3} at 20°C), η is the viscosity of water (1.002 × 10^{-3} Pa • s at 20°C), *CD* is the mean conduit density, and *D* is calculated separately for LW and EW using the following equation (Steppe & Lemeur, 2007):

$$D = \sqrt[4]{\frac{1}{n} \sum_{i=1}^{n} \frac{2a_i^3 b_i^3}{a_i^2 + b_i^2}}, \tag{5}$$

where *n* is the number of conduits measured, and *a* and *b* are the major and minor axes (respectively) of the assumed "ellipse" created by the lumen area.

Vessel implosion resistance (VIR) was calculated as:

$$\text{VIR} = (t/b)_h^2, \quad (6)$$

Where *t* is the double wall thickness and *b* is the conduit wall span. Double wall thickness was measured directly from 1000x magnification images. Conduit wall span was estimated as one side of a square with an area equal to mean conduit area (Hacke et al., 2001).

Budburst Phenology

Budburst monitoring began on 1 March 2022 and ended 28 November 2022. We visually assigned the terminal buds of each juvenile to one of six budburst stages once a week, with stage one being a closed bud and stage six being needle elongation (Figure 5) (Martínez-Berdeja et al., 2019; Ulrich et al., 2023). Budburst stages were tracked using wooden markers of assorted colors for each stage, allowing for quick assessment. Once a juvenile progressed a stage, the wooden marker was changed, and the date was recorded. We calculated the number of days from stage one to each budburst stage.

Physiological Traits

During 15 June 2022 through 28 November 2022, gas exchange, leaf temperature, predawn and midday leaf water potentials (Ψ_{pd}, Ψ_{md}), soil VWC, and a visual health score were measured weekly on each juvenile. Gas exchange was measured using a portable photosynthesis instrument (LI-6800, LI-COR, Lincoln, NE USA) with the cuvette environment set to the following: 1000 μmol m^{-2} photosynthetic photon flux density (saturating light level in the greenhouse), 60% relative humidity, 400 ppm [CO_2], 25 °C leaf temperature, and 500 μmol s^{-1}

flow rate. We selected a cluster of needles (between one to two fascicles) from mature growth of the previous year and taped them together so that they created a flat plane with no overlapping needles. We used the same cluster of needles for gas exchange measurements each week. Following destructive harvest, we measured the total leaf area of these clusters to correct gas exchange measurements for leaf area. Leaf temperature was measured using an infrared thermometer held exactly ten centimeters from the same cluster of needles selected for gas exchange measurements. For predawn and midday leaf water potentials (Ψ_{pd}, Ψ_{md}), we collected two needles from each juvenile once a week at two timepoints: one hour before the projected time of dawn (between 3 am and 6 am as days became shorter) and at 12:30 pm, respectively. Needles were immediately placed on a damp paper towel in a sealed plastic bag and kept on ice between sample collection and measurements. Samples were measured within one hour of being collected using a pressure chamber (PMS Instrument Company, Albany, OR, USA). VWC was measured simultaneously with gas exchange measurements using a HydroSense II Handheld Soil Moisture Sensor (Campbell Scientific, Logan, UT, USA). A visual health score was determined on a subjective scale of 0-5 based on both the coloring (i.e., vivid green, muted green, yellowing, yellow, browning, or dead), maintenance/loss of needles, the turgor of the majority (>80%) of the remaining needles, with zero being dead and five being bright green and healthy.

Volatile Organic Compounds

Whole plant volatile organic compounds (wpVOCs) were measured at three timepoints (one week before treatment (11 June 2022), eleven weeks into the experiment (8 August 2022), and one week before treatment ended (28 November 2022) using the headspace method (Burkle & Runyon, 2017). To measure whole plant VOC emission for each juvenile, we secured a Teflon

bag (50 cm wide x 75 cm deep, American Durafilm Co., Holliston, MA, USA) around the entire aboveground tissue of each juvenile, securing it at the base of the main stem. A volatile trap containing 30 mg of the porous polymer adsorbent HayeSep-Q (Restek, Bellefonte, PA, USA) was inserted into a small opening in the bag and taped into place to seal the opening around the trap. Air was pumped out of the bag through the volatile trap using a vacuum pump (Airlite air sampling pump, SKC Inc., Eighty Four, PA, USA) for a total of 45 min per juvenile. Traps were kept on ice and transported to the U.S. Forest Service, Rocky Mountain Research Station (USFS RMRS) lab in Bozeman, MT, USA, sealed and stored at 4°C, and processed within three weeks of collection. We flushed traps with 200 µL of dichloromethane and a gentle stream of ultra-high-purity nitrogen gas to elute compounds from the volatile trap and added 1 µg of n-nonyl acetate as the internal standard to samples prior to analysis.

Phloem volatile resin (PVR) samples were collected following Runyon et al. (2022) after the experiment ended in December 2022. A 0.5-cm-long section of fresh stem was immediately placed on ice and transported to the USFS RMRS lab. Samples were stored at -80°C prior to analysis. For sample analysis, we removed all the outer bark from each frozen sample prior to removing the phloem. Approximately 25 mg of frozen phloem was then cut into small pieces (~2 mm^3), placed in 1 mL of 95% *n*-Hexane (Sigma-Aldrich, St. Louis, MO; ACS reagent grade), and agitated at room temperature for 24 h. Solvent was then transferred to new vials and an additional 0.25 mL of Hexane was used to rinse the remaining phloem pieces two times, resulting in a final volume of 1.5 mL in the new vials. 100 µg of *n*-nonyl acetate was added as the internal standard to samples prior to analysis. The remaining phloem pieces were placed in a drying oven for one week and weighed to correct the compound concentrations for PVR.

Both processed samples from wpVOCs and PVR were analyzed using an Agilent 7890A gas chromatograph (GC) coupled with a 5975C mass spectrometer and separated on a HP-1ms (30 m x 0.25 mm i.d, 0.25 μm film thickness) column with helium as the carrier gas. Quantifications were made based on the internal standard by using ChemStation software (Agilent Technologies, Wilmington, DE, USA). We used the NIST 08 Mass Spectral Search Program (National Institute of Standards and Technology, Gaithersburg, MD, USA) to identify compounds and confirmed them using commercial standards. We then corrected all values using the total dried biomass of needles and stem for wpVOCs, and the dried biomass of the collected phloem for PVR to give mg of compound per g of dry plant material (stem + needle biomass for wpVOCs and phloem for PVR).

Non-structural Carbohydrates

The concentration and composition of total non-structural carbohydrates (NSCs), glucose, sucrose, fructose, and starch (mg compound/g plant material) were measured separately for roots, stems, and needles of each individual following the enzyme method (Landhäusser et al., 2018). Following the destructive harvest (Table 2), we separated roots, stems (except for the sample of stem used for xylem and phloem analyses), and needles into paper bags, and microwaved the plant tissue for three minutes in one minute intervals to halt enzymatic activity (Landhäusser et al., 2018) (Figure 6). The separated plant tissue was then dried for 72 h at 45°C, and then weighed for biomass traits (described above). Dried and weighed samples were then ground first in a coffee grinder, then to a fine powder using an industrial sample processing grinder (Mixer/mill 8000M, SPEX CertiPrep, Metuchen, New Jersey, USA).

We then conducted an ethanol extraction to release glucose, fructose, and sucrose into solution from the tissue sample. Ethanol was added to tissue sample and boiled at 90°C in a water bath for 10 min. Samples were then centrifuged for 1 min. Supernatant was used for sugar quantification and the remaining pellet was used for starch extraction. Glucose was converted to glucose-6-phosphate through the addition of glucose assay reagent (GHK) and the concentration was measured using a microplate spectrophotometer (μQuant™, BioTek Instruments, Winooski, VT, USA). Sucrose was converted to free glucose by a reaction with invertase, then converted to glucose-6-phosphate using GHK. Total sucrose concentration was calculated as the total glucose-6-phosphate concentration from this reaction minus the total glucose-6-phosphate concentration from the initial glucose reaction. Fructose was converted to fructose-6-phosphate through a reaction with phosphoglucose isomerase (PGI), which was then converted to glucose-6-phosphate by GHK. The concentration of glucose-6-phosphate was measured and again the concentration of glucose was subtracted to determine the concentration of fructose alone. The pellet from the ethanol extraction was washed with ethanol twice more to ensure no remaining soluble sugars altered starch measurements. The pellet was then dried at room temperature for a minimum of 6 h to evaporate any residual ethanol. Starch extraction was accomplished using a two-step process: first, starch was converted to water-soluble glucans with the addition of α-amylase, then glucans was converted to free glucose through a reaction with amyloglucosidase (AMG). Free glucose was then converted to glucose-6-phosphate using GHK and the concentration was measured. NSC concentrations are presented in % of dry weight.

Statistical Analysis

All analyses were conducted in R (R Core Team, 2023). For climate analyses that compared PIAL vs PIBA, PIAL vs $PIBA_N$, PIAL vs $PIBA_S$, and $PIBA_N$ vs $PIBA_S$, we used 30-year-normal monthly climate data from Prism Climate Group including the following climate variables: mean precipitation, total precipitation, minimum precipitation, maximum precipitation, average minimum temperature, average temperature, average maximum temperature, average dewpoint, average minimum VPD, average maximum VPD, average VPD, maximum temperature, minimum temperature, and temperature range (PRISM Climate Group at Oregon State University, 2020) (Table 1). We used these data to calculate annual means for each climatic variable and means for the growing season (March – August) and winter season (September-February). We ran ANOVAs to identify significant differences in climate variables means between groups (PIAL vs PIBA, PIAL vs $PIBA_N$, PIAL vs $PIBA_S$, and $PIBA_N$ vs $PIBA_S$) and calculated estimated differences using Tukey's Honest Significant Difference test at family-wise error rate of 0.05.

For morphological and biomass, stomatal, xylem, budburst, and NSCs, we used linear mixed effects models and *post hoc* linear contrasts (*lme4, emmeans* v1.8.8) to estimate marginal mean differences between drought and control treatments, PIAL vs PIBA, PIAL vs $PIBA_N$, PIAL vs $PIBA_S$, and $PIBA_N$ vs $PIBA_S$, with treatment (drought, control), family (Jefferson, Burke, and Big Mountain for PIAL, '267' and '330' for $PIBA_N$, and '296' and '314' for $PIBA_S$), and species (PIAL, PIBA) as fixed effects and bin number as a random effect. For physiological traits (A, g_s, Ψ_{pd}, Ψ_{md}, Ψ_{md}- Ψ_{pd}, T_{leaf}), we used the above-described model with date as an additional fixed

effect and both bin number and tree ID (as there were weekly repeated measures for these traits) as random effects.

For wpVOCs and PVR compounds, we used random forest analysis to identify influential compounds. Specifically, we used five random forest models with all identified compounds as predictors and one of the following as a response variable for each model: 1) control vs drought, 2) PIAL vs PIBA, 3) PIAL vs $PIBA_N$, 4) PIAL vs $PIBA_S$, and 5) $PIBA_N$ vs $PIBA_S$. We then calculated mean decrease accuracy where compounds with higher mean decrease accuracy represented a higher loss of accuracy should that variable be removed from the model (i.e. mean decrease accuracy is a metric of how influential each compound is in predicting the response variable, so that a higher mean decrease accuracy indicates higher influence). We selected the top four compounds from each of the tests to create a list of influential compounds for wpVOCs and a separate list for PVR compounds for our five comparisons (1) drought and control groups, 2) PIAL and PIBA, 3) PIAL and $PIBA_N$, 4) PIAL and $PIBA_S$, and 5) $PIBA_N$ and $PIBA_S$. To estimate mean marginal differences of these influential compounds for each comparison, we ran mixed linear models and *post hoc* linear contrasts (lme4 v 1.1.34, emmeans v1.8.8) with treatment, family, and species as fixed effects and bin number as a random effect. For the wpVOCs, where data were collected at three different timepoints, we also included date and tree ID as random effects. Additionally, we created non-metric multidimensional scaling (NMDS) plots using Bray-Curtis dissimilarity matrices to visualize differences between groups.

RESULTS

PIAL vs PIBA

Both PIBA populations originated from seed sources with warmer climates (higher mean temperature and maximum temperature both annually and for Sep-Feb), higher winter precipitation (total precipitation for Sep-Feb), but higher VPD (minimum VPD, maximum VPD, mean VPD annually, Mar-Aug, and Sep-Feb) than those of PIAL (Figure 7; Appx. Table 1). For morphology traits, in comparison to PIAL, PIBA exhibited significantly smaller stem and branch diameters, smaller branch diameter:branch length, taller stems, and smaller stem diameter:stem height (Figure 8). Additionally, PIAL had significantly higher LMA (leaf mass per area) and total canopy area (leaf + woody tissue) than PIBA, while PIBA had significantly lower STAR (sunlit leaf area to total leaf area ratio) than PIAL. In contrast, PIAL and PIBA did not significantly differ in fascicle density, mean branch length, branch diameter:stem diameter, total leaf area, LA:SA (leaf area:sapwood area), or any biomass measurements (Appx. Table 2). For stomatal traits, PIBA had significantly larger aperture area, aperture length, and guard cell area than PIAL, but stomatal density and total number of stomata did not significantly differ between species. For xylem traits, PIBA had significantly higher LW tracheid density and EW cell wall thickness than PIAL, and significantly smaller mean LW lumen area and marginally lower K_p (potential conductivity) than PIAL. Also, PIBA had significantly higher resin duct density (Figure 8) but smaller mean resin duct area than PIAL. In contrast, PIAL and PIBA did not significantly differ in any ring width measurements, EW lumen area, EW tracheid density, cell wall thickness for either EW or LW, or VIR (Vessel Implosion Resistance). For budburst phenology traits, PIAL exhibited significantly earlier budburst than PIBA for stages 2, 3, and 6.

We found no significant differences between species for any measured physiological traits. Influential wpVOCs (whole plant volatile organic compounds) driving the separation between species were: β-Pinene, Unknown Benzene 1, D-Limonene, and Unknown Sesquiterpene 5. Influential PVR (phloem volatile resin) compounds driving the separation between species were: α-Pinene, Limonene, Unknown Sesquiterpene 21, Unknown Sesquiterpene 22 (Table 2). Of the influential wpVOCs, PIAL had significantly lower concentrations of β-Pinene and significantly higher concentrations of Unknown Sesquiterpene 5 that PIBA, but Unknown Benzene 1 or D-Limonene concentrations did not significantly differ between species. Of the influential PVR compounds, PIBA had significantly higher concentrations of α-Pinene, and significantly lower concentrations of Limonene and Unknown Sesquiterpenes 21 and 22. However, total wpVOC and PVR compound concentrations did not significantly differ between species. In the NMDS plot of all wpVOCs, we observed overlap PIAL, $PIBA_N$, and $PIBA_S$, creating a transitional gradient from PIAL to $PIBA_N$ to $PIBA_S$ with $PIBA_N$ overlapping with the other two groups, and more separation between PIAL and $PIBA_S$ (Figure 9). In contrast, for PVR, we observed clear separation between PIAL and PIBA where $PIBA_N$ and $PIBA_S$ grouped together with only slight separation between populations (Figure 10). For NSCs (non-structural carbohydrates), PIBA had significantly higher concentrations of needle and stem glucose, needle sucrose, needle and stem soluble sugars (glucose + fructose + sucrose), stem combined glucose + fructose and stem total NSC (glucose + fructose + sucrose + starch) than PIAL (Figure 8). NSC concentrations in roots and starch concentrations in all tissue types did not significantly differ between species.

PIAL vs $PIBA_N$

In comparison to PIAL, $PIBA_N$ exhibited significantly smaller stem diameter:height and total canopy area (Figure 8; Appx. Table 2), while $PIBA_N$ and PIAL did not significantly differ in the other morphology traits (stem diameter, stem height, fascicle density, mean branch diameter, mean branch length, branch diameter:branch length, branch diameter:stem diameter, total leaf area, LMA, LA:SA, STAR, biomass traits). For stomatal traits, $PIBA_N$ had significantly larger aperture area and aperture length than PIAL, but did not have significantly different guard cell areas, stomata density, or total number of stomata. For xylem traits, PIAL had significantly larger resin duct area than PIBA, but not significantly different resin duct density (Figure 11). EW cell wall thickness was thicker in $PIBA_N$ than PIAL. However, K_p, ring width traits, EW and LW lumen area, EW and LW tracheid density, LW cell wall thickness, and VIR did not significantly differ between PIAL and $PIBA_N$. For budburst traits, $PIBA_N$ reached stage 2 significantly earlier than PIAL, while no significant differences were observed for the other five budburst stages. PIAL and $PIBA_N$ did not significantly differ for any physiological traits. Influential wpVOCs driving the separation between PIAL and $PIBA_N$ were: β-Pinene, Unknown Benzene 1, and Unknown Sesquiterpenes 5 and 7 (Table 2). Influential PVR compounds driving the separation between PIAL and $PIBA_N$ were: α-Pinene, Limonene, Unknown Sesquiterpene 4, and Unknown Sesquiterpene 22. Of the influential wpVOCs, PIAL did not significantly differ from $PIBA_N$ for any of the four compounds. Of the influential PVR compounds, $PIBA_N$ had significantly higher concentrations of Unknown Sesquiterpene 4 than PIAL, but did not significantly differ for the other three compounds. $PIBA_N$ did not significantly differ in total wpVOCs and PVR concentrations. WpVOCs did not clearly separate between PIAL and $PIBA_N$

(Figure 9), but PVR compounds did clearly separate between PIAL and $PIBA_N$ (Figure 10). $PIBA_N$ had significantly higher glucose, combined glucose + fructose, and total NSC concentrations in stem tissue than PIAL (Figure 11), while no other stem NSC concentrations differed between $PIBA_N$ and PIAL. PIAL and $PIBA_N$ also did not significantly differ in needle and root NSC concentrations.

PIAL vs $PIBA_S$

In comparison to PIAL, $PIBA_S$ had significantly smaller stem diameter, greater stem length (similar to PIAL vs $PIBA_N$), and smaller stem diameter:stem height (Figure 8; Appx. Table 2). In contrast to PIAL vs $PIBA_N$, LMA and total canopy area were significantly higher in PIAL than $PIBA_S$. $PIBA_S$ had significantly lower STAR and higher LA:SA than PIAL. Similar to the comparison between PIAL and $PIBA_N$, PIAL did not significantly differ from $PIBA_S$ in fascicle density, mean branch diameter, mean branch length, branch diameter:branch length, branch diameter:stem diameter, total leaf area or any biomass traits. For stomatal traits, $PIBA_S$ had significantly larger aperture area and guard cell area than PIAL, but did not significantly differ in aperture length, stomata density, or total stomata number. None of the xylem, budburst phenology, and physiological traits significantly differed between $PIBA_S$ and PIAL. Influential wpVOCs driving the separation between $PIBA_S$ and PIAL were: β-Pinene, Unknown Benzene 1, Unknown Monoterpene 1, and 3-Carene . Influential PVR compounds driving the separation between $PIBA_S$ and PIAL were: Terpinolene, γ-Terpinene, Methyl-thymyl-ether, and Sabinene. These results were similar to the comparison between $PIBA_N$ and PIAL for wpVOCs which also identified β-Pinene and Unknown Benzene 1 as influential. However, these results differ from the comparison between $PIBA_N$ and PIAL for PVR compounds, which did not identify any of the

same above compounds. Of the influential wpVOCs, $PIBA_S$ had significantly higher concentrations of β-Pinene and Unknown Benzene 1 than PIAL, while Unknown Monoterpene 1 and 3-Carene did not significantly differ between PIAL and $PIBA_S$. Of the influential PVR compounds, $PIBA_S$ had significantly higher concentrations of Methyl-thymyl-ether than PIAL but did not significantly differ from $PIBA_S$ in the other three influential compounds. $PIBA_S$ had significantly higher wpVOC total concentration than PIAL, but total PVR compound concentration did not significantly differ between $PIBA_S$ and PIAL. Unlike PIAL vs $PIBA_N$, the NMDS plot showed clear separation between PIAL and $PIBA_S$ for both wpVOCs (Figure 9), and for PVR compounds (Figure 10). $PIBA_S$ and PIAL did not significantly differ for any NSC component in any tissue (Figure 11).

$PIBA_N$ vs $PIBA_S$

Comparing $PIBA_N$ to $PIBA_S$ population locations, $PIBA_N$ had significantly higher total annual precipitation and lower elevation than $PIBA_S$, but no significant differences were found for any other climate variables (Table 1; Appx. Table 1). Unlike comparisons between species or PIAL and each PIBA population, there were very few significant trait differences between $PIBA_N$ and $PIBA_S$. Of all morphology, stomatal, xylem, budburst, and physiology traits, only LA:SA was significantly higher in $PIBA_S$ than in $PIBA_N$, and EW cell wall thickness was significantly thicker in $PIBA_N$ than in $PIBA_S$ (Appx. Table 2). Influential wpVOCs driving the separation between $PIBA_N$ to $PIBA_S$ were: β-Pinene, Unknown Sesquiterpene 5, Unknown Monoterpene 1, and 3-Carene. Influential PVR compounds driving the separation between $PIBA_N$ to $PIBA_S$ were: α-Pinene, Limonene, Terpinolene, and Sabinene. Of the influential wpVOCs, $PIBA_S$ had significantly higher concentrations of β-Pinene than $PIBA_N$, but the two

populations did not significantly differ in concentrations of 3-Carene, Unknown Sesquiterpene 5, or Unknown Monoterpene 1. None of the influential PVR compounds significantly differed between populations. $PIBA_S$ had significantly higher total concentrations of PVR compounds while wpVOC concentration did not significantly differ between populations. The NMDS plot showed no clear separation for either wpVOCs (Figure 9) or PVR compounds (Figure 10). $PIBA_S$ and $PIBA_N$ did not significantly differ in any NSC component in any tissue type.

Drought vs Control

We observed very few significant trait differences between species-specific responses to treatments. Overall, across both species, the drought treatment had an 18% lower soil volumetric water content than the control treatment. Out of all morphology, stomatal, xylem, budburst, physiology, and NSC traits, only four traits differed significantly: drought LA:SA and guard cell area were significantly higher than control for PIBA but not for PIAL, and drought LW ring width was significantly greater and root starch concentration was significantly lower than control for PIAL but not for PIBA. Influential wpVOCs driving the separation between treatments for both species were: Unknown Sesquiterpene 5, Unknown Monoterpenes 3 and 4, and β-ocimene-2. Influential PVR compounds driving the separation between treatments for both species were: Sabinene and Unknown Sesquiterpenes 3, 4, and 20. Of the influential wpVOCs, control had significantly higher concentrations of Unknown Monoterpenes 3 and 4 than drought for PIBA but not for PIAL, while Unknown Sesquiterpene 5 or β-ocimene-2 did not significantly differ between treatments for either species. We found no significant differences in any of the four influential PVR compounds for either species. Drought concentrations of total wpVOCs were

significantly lower than control for PIBA but not for PIAL while total PVR concentration did not significantly differ between treatments for either species.

DISCUSSION

PIAL and PIBA displayed different suites of traits that enable them to persist in their high elevation habitats which are characterized by similar abiotic stressors (cold temperatures, high winds, summer drought) and biotic stressors (white pine blister rust, bark beetle). For most of our measured traits, PIAL and $PIBA_S$ differed the most. In contrast, $PIBA_N$ was similar to both groups, and often was intermediate between PIAL and $PIBA_S$. Although $PIBA_N$ and $PIBA_S$ were similar for most traits, they differed most notably in wpVOC characteristics, where $PIBA_S$ had significantly higher total wpVOC concentration than $PIBA_N$. Our drought treatment did not induce measurable physiological drought responses, so we have focused the Discussion on comparing traits of PIAL, $PIBA_N$, and $PIBA_S$.

PIAL and PIBA Displayed Different Suites of Traits for Responding to Abiotic and Biotic Stress

Between the two species, PIAL and PIBA displayed different groups of traits that enable them to withstand mechanical stress from high winds and to resist drought, common abiotic stressors in the exposed, high-elevation habitats of these pines. Compared to PIBA, PIAL had shorter, thicker stems, higher stem diameter:stem height, and higher branch diameter:branch length, traits that increase stem and branch mechanical strength (Table 2, Figure 8) (Read & Stokes, 2006; Ulrich et al., 2023b). PIBA had significantly smaller and more densely packed LW (latewood) tracheids than PIAL, which is a common strategy that fortifies stems to withstand physical damage (Brodribb et al., 2017; Domec & Gartner, 2002; Zhong et al., 2020). Consistently, we observed that PIBA had significantly taller stems than PIAL. A consequence of PIBA's smaller, densely packed LW tracheids relative to PIAL's was a significantly lower K_p

(potential hydraulic conductivity), the total amount of water that can theoretically be transported through the stem, compared to PIAL, highlighting the classic trade-off between hydraulic safety and hydraulic efficiency (Lachenbruch & McCulloh, 2014; McCulloh et al., 2019). Wider tracheids increase the efficiency of water transport throughout the plant (more 'efficient'), thereby increasing rates of photosynthesis, growth, and metabolism (Fu et al., 2019). However, wider tracheids also are more vulnerable (less 'safe') to embolism (air bubbles that obstruct water transport), which can result in hydraulic failure (Brodribb et al., 2017). Therefore, PIBA's smaller and densely packed LW tracheids increase hydraulic safety, thereby increasing PIBA's drought resistance. However, this increased hydraulic safety comes at the expense of reduced hydraulic efficiency, commonly observed in drought-adapted species (Brodribb et al., 2017; Fu et al., 2019; Lachenbruch & McCulloh, 2014). Like PIBA, PIAL also displayed drought resistance but with different traits. Specifically, compared to PIBA, PIAL exhibited higher LMA (leaf mass per area) and smaller stomatal (aperture) size, both of which reduce foliar water loss, increasing PIAL's drought tolerance (Bertolino et al., 2019; Neyret et al., 2016; Poorter et al., 2009; Reich et al., 1997; Wright et al., 2004; Wright & Westoby, 2002; H. Yang & Wang, 2001). Additionally, higher LMA may increase leaf life span to protect against cold stress (Takahashi & Miyajima, 2008), and may also increase light absorption (Poorter et al., 2009), which is consistent with PIAL's significantly greater total canopy area and lower STAR compared to PIBA.

Xylem traits are often correlated with stomatal traits to support whole plant water transport where liquid water travels through xylem and gaseous water evaporates from stomata. As a result, increased tracheid density and smaller tracheid size or lumen area have been observed in tandem with higher stomatal density and smaller stomata (Aasamaa et al., 2001;

Brodribb et al., 2017; Zheng et al., 2022; Zhong et al., 2020). Just like tracheid size (lumen area), stomatal size has been shown to be positively correlated with water availability, increasing hydraulic efficiency but reducing hydraulic safety (Bertolino et al., 2019; Guérin et al., 2018; Park et al., 2016; Xu & Zhou, 2008; H. Yang & Wang, 2001). We unexpectedly observed that PIBA exhibited significantly larger stomata, smaller LW lumen area, and higher LW tracheid density than PIAL. This could suggest that hydraulic coordination between stomata and xylem traits may not occur in all species. Alternatively, other traits which were not measured in this study may compensate for this unexpected lack of coordination between our measured xylem and stomatal traits. For example, more dynamic traits that describe stomatal kinetics (such as the rate of stomata opening and closing) may more strongly coordinate with xylem traits, as stomatal size and density are relatively static traits (Brodribb et al., 2017; Drake et al., 2013; Letts et al., 2009).

PIBA had significantly higher concentrations of needle and stem soluble sugars (glucose, fructose, and sucrose) than PIAL, suggesting that compared to PIAL, PIBA may be better adapted to respond to immediate onset of environmental stress such as drought or pests, which may be more likely to occur during PIBA's longer and warmer growing season than PIAL's (Schoettle et al., 2022b) (Table 1, Figure 7). To understand plant NSC dynamics, we will use the analogy of NSCs as a plant's financial "currency" that can be spent on various functions crucial for plant survival: growth, maintenance, storage, defense, or reproduction (El Omari, 2022; Huang et al., 2019). NSCs and financial currency are both limited resources that come in different forms (soluble sugars, starch; cash, savings account) and must be allocated or budgeted strategically to survive environmental or financial stress. Once NSCs and currency are allocated

to or spent on one function, they are no longer available and reduce the individual's total NSCs or currency available to spend. Soluble sugars (glucose, fructose, sucrose) have low-molecular weight and are easily and quickly transported and allocated to various plant functions, making soluble sugars like cash that can be quickly spent. In contrast, starch is a large storage polysaccharide with higher molecular weight that must be broken down into soluble sugars before it can be used and can therefore be considered like a savings bank account that requires extra steps to spend those NSCs or currency (Landhäusser et al., 2018). High starch stores or a full savings account better prepares individuals for future or prolonged environmental or financial stress but cannot be used to quickly respond to immediate environmental or financial crisis. In contrast, if an individual's NSCs or currency are in the form of soluble sugars or cash on-hand, they can survive immediate environmental or financial stress but are also more likely to deplete those sugars or cash before stress is relieved. How plants allocate their NSCs to sugars and starch is critical for withstanding environmental stress. For example, since NSCs can be allocated and converted to defense compounds, PIBA's higher soluble sugar concentrations may yield higher levels of defense compounds such as wpVOCs and PVR compounds than PIAL (Bryant et al., 1983; Herms & Mattson, 1992; Huang et al., 2019) (described below).

Although total concentrations of wpVOCs (whole plant volatile organic compounds) and PVR (phloem volatile resin) compounds did not significantly differ between species, PIAL and PIBA significantly differed in concentrations of 8 of the 16 identified influential wpVOCs and PVR compounds, suggesting that each species may be able to respond to stress with species-specific compounds. VOCs are defense compounds that protect against herbivory, pests, and pathogens and are created in a process that requires the metabolism of NSCs (Bryant et al., 1983;

Herms & Mattson, 1992; Runyon et al., 2020). Of the 8 compounds identified as influential for driving species differences, PIAL had significantly higher concentrations of Unknown Sesquiterpene 5 (wpVOCs), and Limonene, Sabinene, and Unknown Sesquiterpenes 21, and 22 (PVR) than PIBA, while PIBA had significantly higher concentrations of β-Pinene and Unknown Monoterpene 3 (wpVOCs) and Unknown Sesquiterpene 4 (PVR) (Table 2). In PIAL and PIBA, wpVOCs and PVR may protect against bark beetles such as Mountain Pine Beetle (*Dendrotonus ponderosae* Hopkins).

To our knowledge, this is the first study to measure wpVOCs and PVR in PIBA and PIAL juveniles. Previous studies have measured wpVOCs and PVR in mature, adult trees in the field, which found significantly higher total concentrations of both wpVOCs and PVR compounds in PIBA than in PIAL (Runyon et al., 2020). This contrasts with our finding that wpVOC and PVR compound concentrations did not significantly differ between species, highlighting that adults and juveniles may respond to or be affected by stress in different ways. For example, mountain pine beetles only infest mature adult trees, while seedlings and juveniles are not at risk of attack (Bentz et al., 2016a, 2022). We did however identify β-pinene, 3-carene, Unknown Monoterpene 1, and Unknown Sesquiterpene 5 in juveniles that were also identified in adults of PIBA and PIAL in Runyon et al. 2020, suggesting that juvenile defense mechanisms may underlie adult defense mechanisms. For example, we found that resin duct density was significantly higher in PIBA juveniles than PIAL juveniles, which may be a precursor to adult defense against bark beetles because resin ducts are permanently embedded into the stem. Resin is synthesized and stored within resin ducts in coniferous species and functions as both a physical and chemical defense mechanism (Mason et al., 2019). Larger resin ducts have correlated with higher

concentrations of certain PVR compounds in PIAL while increased resin duct density had variable effects depending on the compound (Mason et al., 2019). Resin duct density is considered a proxy for functional defense against pathogens and pests (Hood et al., 2020). Because both VOCs and PVR compounds also protect against herbivory, microbial pathogens, and abiotic stress like heat and cold, further research should compare secondary metabolite concentration between juveniles and adult trees of the same species in the field.

Traits of PIAL Differed More from $PIBA_S$ than $PIBA_N$

For the majority of our measured traits, PIAL and $PIBA_S$ differed the most while $PIBA_N$ was the intermediate between $PIBA_S$ and PIAL, suggesting that $PIBA_S$ was likely driving our observed significant trait differences between species. This transitional gradient in trait values from PIAL to $PIBA_N$ to $PIBA_S$ was most strongly observed in our NMDS analysis of wpVOCs where PIAL and $PIBA_S$ clearly separated, while $PIBA_N$ was the intermediate that overlapped with both groups. In contrast to wpVOCs, for PVR compounds, we observed complete separation between both PIBA populations and PIAL. Interestingly, we also observed this transitional gradient from PIAL to $PIBA_N$ to $PIBA_S$ in other traits including stem diameter, stem height, stem diameter:stem height, LMA, STAR, canopy area, aperture area, guard cell area, total wpVOC concentration, and needle soluble sugar concentrations (Figure 11), all of which significantly differed between PIAL and $PIBA_S$. We hypothesize that PIAL was more similar to $PIBA_N$ than $PIBA_S$ because PIAL and $PIBA_N$ originated from locations closer in latitude, which may contribute to PIAL and $PIBA_N$ having similar growing season mean temperatures, where $PIBA_N$ had warmest growing season temperatures, PIAL had moderate growing season temperatures, and $PIBA_S$ had the coolest growing season (Appx. Table 1). Based on latitude

alone, these temperature patterns were unexpected but can be explained by elevation being highest in $PIBA_S$, followed by $PIBA_N$, and then PIAL being lowest (Table 1). Additionally, PIAL and $PIBA_N$ had similar annual and growing season (Mar-Aug) mean precipitation, while $PIBA_S$ had significantly lower mean precipitation. However, not all climate variables support this hypothesis; for example, winter precipitation (Sep-Feb) significantly differed different between PIAL and $PIBA_N$, while PIAL and $PIBA_S$ had similar levels of winter precipitation.

$PIBA_S$ Had Higher VOC Concentrations than $PIBA_N$

Unlike the previous between-species comparisons, we found very few within-species population differences between $PIBA_N$ and $PIBA_S$ despite that some trait comparisons with PIAL differed between each population. Only a few traits significantly differing between populations was consistent with only one climate variable, total precipitation, significantly differing between the two PIBA populations. Because $PIBA_N$ had significantly higher levels of total precipitation than $PIBA_S$, we had hypothesized that $PIBA_S$ would exhibit more drought-resistant traits than $PIBA_N$. This was supported by two traits that significantly differed between populations, LA:SA and EW cell wall thickness. $PIBA_S$ had significantly higher LA:SA than $PIBA_N$. LA:SA is expected to decrease with decreasing water availability because lower LA:SA reduces the leaf area through which water can be lost through transpiration (Togashi et al., 2015). Additionally, $PIBA_N$ had significantly higher EW cell wall thickness than $PIBA_S$, which can increase hydraulic efficiency and water transport, which may occur due to increased water availability in $PIBA_N$'s climate of origin.

In addition to LA:SA and EW cell wall thickness, $PIBA_S$ had significantly higher concentrations of total wpVOC and β-pinene than $PIBA_N$. Higher temperatures have been linked to higher concentrations of wpVOCs in PIBA and PIAL (Runyon et al., 2020). Therefore, our result was unexpected because the climate of $PIBA_S$ is marginally colder than that of $PIBA_N$. We hypothesize that $PIBA_S$'s higher concentrations of total wpVOC and β-pinene could occur if $PIBA_S$ is able to emit higher rates of wpVOCs under non-stressful temperatures, which was the case in our common environment study. WpVOC concentrations (and other traits) may differ between stressful and non-stressful conditions (Deslauriers et al., 2019; Duan et al., 2018). Additionally, both structural and chemical defense traits have been linked to historical exposure to pests and pathogens (Mason et al., 2019), suggesting that higher levels of wpVOC concentrations in $PIBA_S$ than $PIBA_N$ may indicate exposure to different pests or pathogens in the past, which may be a heritable and population-specific trait.

Drought Treatment Did Not Induce Physiological Response

Although the drought treatment resulted in 18% lower VWC than the control treatment, neither pre-dawn nor midday leaf water potentials (metrics of plant water status) differed significantly between treatments when species was accounted for in our linear mixed effects models, suggesting that the drought treatment did not induce a measurable physiological response in our study trees. In addition, g_s (stomatal conductance) and A (photosynthesis) also did not differ significantly between drought and control treatments. Of all traits measured, LA:SA in PIBA, guard cell area in PIBA, LW ring width in PIAL, and root starch concentration in PIAL were the only traits that significantly differed between treatments. While root starch was lower in droughted PIAL than control PIAL and could indicate drought-induced NSC depletion,

the other three significant differences are unlikely to be biologically meaningful or to have been caused by drought treatment due to the slow growing nature of our species. Additionally, with only four significant differences out of 194 total trait comparisons, significant differences are likely to be the result of spurious correlation, especially as physiological measurements did not differ between treatments. As a result, we focused our analyses on comparing traits between species and populations.

The minimal effect of our drought treatment most likely occurred due to the method we used for droughting. We had selected the Marchin et al., 2020 drought method to create a long-term moderate drought that was representative of field conditions. However, the method was originally developed on tropical plant species which are more adapted to utilizing surface water that is more readily available in tropical climates (Marchin et al., 2022). In contrast, both PIBA and PIAL species have deeper root systems to access water deep in the soil when precipitation is scarce (Campbell et al., 2011). Consistently, members of *Pinus* are known for their ability to draw water from deeper soil at higher rates than many other species (such as *P. sylvestris* in China and *P. caribaea* in Sri Lanka) to an extent that managers in Africa and many Asian countries aim to remove *Pinus* trees because of their negative effects on groundwater recharge (Piyaruwan et al., 2020; Tuswa et al., 2019; Wang et al., 2008). Most likely, the juveniles in this study more efficiently drew water through the soil through the floral foam, allowing constant access to water even in the drought treatment. Additionally, because both PIAL and PIBA are slow-growing species that are already adapted to prolonged periods of drought, they use water and dry out the soil more slowly than the tropical plants used originally in the Marchin et al., 2020 method. Future greenhouse drought experiments with high-elevation *Pinus* should consider

fully withholding water as a means of implementing drought stress rather than trying to moderate the amount of available water.

Conclusions

In this study, PIAL and PIBA displayed different suites of traits that enable them to persist in their high elevation habitats, characterized by similar abiotic stressors (cold temperatures, high winds, summer drought) and biotic stressors (white pine blister rust, bark beetle). For most of our measured traits, PIAL and $PIBA_S$ differed the most while $PIBA_N$ was the intermediate being more similar to both groups, especially in wpVOC composition. $PIBA_N$ and $PIBA_S$ were similar for most traits but differed most notably in wpVOC concentration. Although our drought treatment did not induce a measurable physiological response, we learned that fully withholding water may have been the most effective method for successfully droughting these species.

The results of this study can only be inferred to the represented families for both PIAL and PIBA, as juveniles were randomly sampled from these families only. Our results are specific to the juvenile life stage for these two species and will likely differ from similar studies conducted on adult trees in the field. However, it is important to understand both juvenile and adult physiology and morphology in order to create a complete picture of future species distributions, as no tree can reach mature, reproductive age without first surviving the juvenile stage. Additionally, because this study was conducted in a controlled greenhouse environment and not in the field, we cannot make direct inferences to field-grown juveniles. Our common environment experiment in a controlled greenhouse allowed us to identify trait differences

between species and populations and to attempt to implement an experimental drought treatment without confounding factors that arise in field studies. Although the drought treatment was ineffective, our study improves our understanding of the physiological mechanisms that contribute to PIAL's and PIBA's abilities to inhabit high elevations where no other tree types persist. Our physiological characterization of PIAL and PIBA helps us better predict how and where future climates may affect these special species.

With climate change and anthropogenic disturbances causing shifts in species distributions and forest species compositions, investigating and comparing species- and population-specific physiological and morphological traits can help us understand and predict future forest species distributions. Investigating such traits reveals mechanisms for how a tree interacts with and responds to its environment and survives abiotic and biotic stress. Species- and population-specific traits may result from phenotypically plastic adjustments or heritable genetic adaptation. Using common environment studies such as ours, we can identify traits that are the result of genetic selection (those that significantly differ between species or populations), and studying these traits can help us understand species survival strategies under future climates. From our study, we found that, although similar in many ways, PIAL and PIBA, as well as the populations of PIBA, have different suites of traits that allow them to respond and adapt to stress through unique strategies, meaning that changing climates will continue to affect these trees in different ways.

TABLES AND FIGURES

Tables

Table 1: Species (whitebark pine, PIAL; foxtail pine, PIBA), family seed source location (latitude (LAT), longitude (LON), Fig. 1), and climate (precipitation (mm), temperature (°C), VPD (hPa)) from 1991-2020 (Prism Climate Group, 2020; 800m resolution) for annual, growing season (March-August), and winter (September-February) timeframes.

	Species	PIAL			PIBA			
	Population				North PIBA ($PIBA_N$)		South PIBA ($PIBA_S$)	
	Family	BIGMTN	BURKE	JEFF	267	330	296	314
	LAT (°)	46.87	48.50	47.52	41.22	41.33	35.93	36.38
	LON (°)	-110.66	-114.35	-115.71	-122.80	-122.60	-118.30	-118.50
	Elevation (m)	2290.00	1860.00	1930.00	2103.00	2397.00	2834.00	2987.00
Annual	Mean Precipitation	108.99	112.72	71.22	170.08	143.43	69.63	98.23
	Total Precipitation	1307.83	1352.60	854.61	2041.00	1721.19	835.61	1178.80
	Minimum Precipitation	37.08	30.06	48.04	15.66	13.06	8.44	8.24
	Maximum Precipitation	160.78	178.67	107.00	374.84	275.84	151.82	217.49
	Average Minimum Temperature	-2.29	-0.32	-3.99	1.18	1.53	-0.63	-2.38
	Average Temperature	2.48	4.03	1.97	5.88	6.36	5.36	3.53
	Average Maximum Temperature	7.26	8.37	7.95	10.58	11.21	11.37	9.46
	Average Dewpoint	-3.63	-1.62	-4.78	-2.78	-2.62	-4.78	-7.08
	Average Minimum VPD	1.55	1.63	1.06	2.69	2.82	2.64	2.54
	Average Maximum VPD	6.55	7.00	7.74	9.43	9.80	10.81	9.99
	Average VPD	4.05	4.31	4.40	6.06	6.31	6.73	6.27

	Maximum Temperature	21.20	22.10	21.90	21.40	22.40	21.20	18.30
	Minimum Temperature	-9.80	-7.70	-12.20	-5.40	-4.20	-7.80	-9.20
	Temperature Range	31.00	29.80	34.10	26.80	26.60	29.00	27.50
Growing Season (Mar-Aug)	Mean Precipitation	82.77	67.74	75.61	59.32	56.89	24.97	34.66
	Total Precipitation	496.60	406.45	453.68	355.89	341.35	149.82	207.95
	Minimum Precipitation	37.08	30.06	48.04	15.66	13.06	8.44	8.24
	Maximum Precipitation	133.24	109.48	107.00	139.88	138.31	65.30	98.27
	Average Minimum Temperature	2.87	4.73	1.52	4.83	5.43	3.55	1.78
	Average Temperature	8.95	10.22	8.42	10.40	11.05	9.85	7.85
	Average Maximum Temperature	15.05	15.70	15.32	15.93	16.70	16.18	13.93
	Average Dewpoint	0.43	2.08	0.02	0.08	0.17	-0.92	-3.20
	Average Minimum VPD	2.36	2.79	1.48	3.90	4.18	3.60	3.50
	Average Maximum VPD	10.52	11.47	11.91	13.67	14.22	14.20	13.12
	Average VPD	6.44	7.13	6.69	8.79	9.20	8.90	8.31
	Maximum Temperature	21.20	22.10	21.90	21.40	22.40	21.20	18.30
	Minimum Temperature	-4.30	-2.70	-6.30	-2.90	-2.20	-4.90	-6.30
	Temperature Range	25.50	24.80	28.20	24.30	24.60	26.10	24.60
Winter Season (Sep-Feb)	Mean Precipitation	135.21	157.69	66.82	280.85	229.97	114.30	161.81
	Total Precipitation	811.23	946.15	400.93	1685.11	1379.84	685.79	970.85
	Minimum Precipitation	96.45	118.67	62.68	95.65	96.71	31.18	48.47
	Maximum Precipitation	160.78	178.67	73.25	374.84	275.84	151.82	217.49
	Average Minimum Temperature	-7.45	-5.37	-9.50	-2.47	-2.37	-4.82	-6.55
	Average Temperature	-4.00	-2.17	-4.48	1.37	1.67	0.87	-0.80
	Average Maximum Temperature	-0.53	1.03	0.58	5.22	5.72	6.55	4.98
	Average Dewpoint	-7.70	-5.32	-9.57	-5.65	-5.40	-8.63	-10.97

	Average Minimum VPD	0.74	0.47	0.64	1.49	1.46	1.68	1.58
	Average Maximum VPD	2.58	2.52	3.57	5.19	5.39	7.43	6.86
	Average VPD	1.66	1.50	2.10	3.34	3.43	4.55	4.22
	Maximum Temperature	6.60	8.10	7.80	11.90	12.70	12.40	10.80
	Minimum Temperature	-9.80	-7.70	-12.20	-5.40	-4.20	-7.80	-9.20
	Temperature Range	16.40	15.80	20.00	17.30	16.90	20.20	20.00

Table 2: The top four influential compounds for each comparison (PIAL vs PIBA, PIAL vs $PIBA_N$, PIAL vs $PIBA_S$, $PIBA_N$ vs $PIBA_S$). Bolded compounds significantly differed ($p \leq 0.05$).

	PIAL vs PIBA	PIAL vs $PIBA_N$	PIAL vs $PIBA_S$	$PIBA_N$ vs $PIBA_S$
Whole Plant Volatile Organic Compounds (wpVOCs)	**β-Pinene**	β-Pinene	**β-Pinene**	**β-Pinene**
	Unknown Benzene 1	Unknown Benzene 1	**Unknown Benzene 1**	
	D-limonene			
	Unknown Sesquiterpene 5	Unknown Sesquiterpene 5		Unknown Sesquiterpene 5
		Unknown Sesquiterpene 7		
			Unknown Monoterpene 1	Unknown Monoterpene 1
			3-Carene	3-Carene
Phloem Volatile Resin (PVR) compounds	**α-Pinene**	α-Pinene		α-Pinene
	Limonene	Limonene		Limonene
		Unknown Sesquiterpene 4		
	Unknown Sesquiterpene 21			
	Unknown Sesquiterpene 22	Unknown Sesquiterpene 22		
			Terpinolene	Terpinolene
			γ-Terpinene	
			Methyl-thymyl-ether	
			Sabinene	Sabinene

Figures

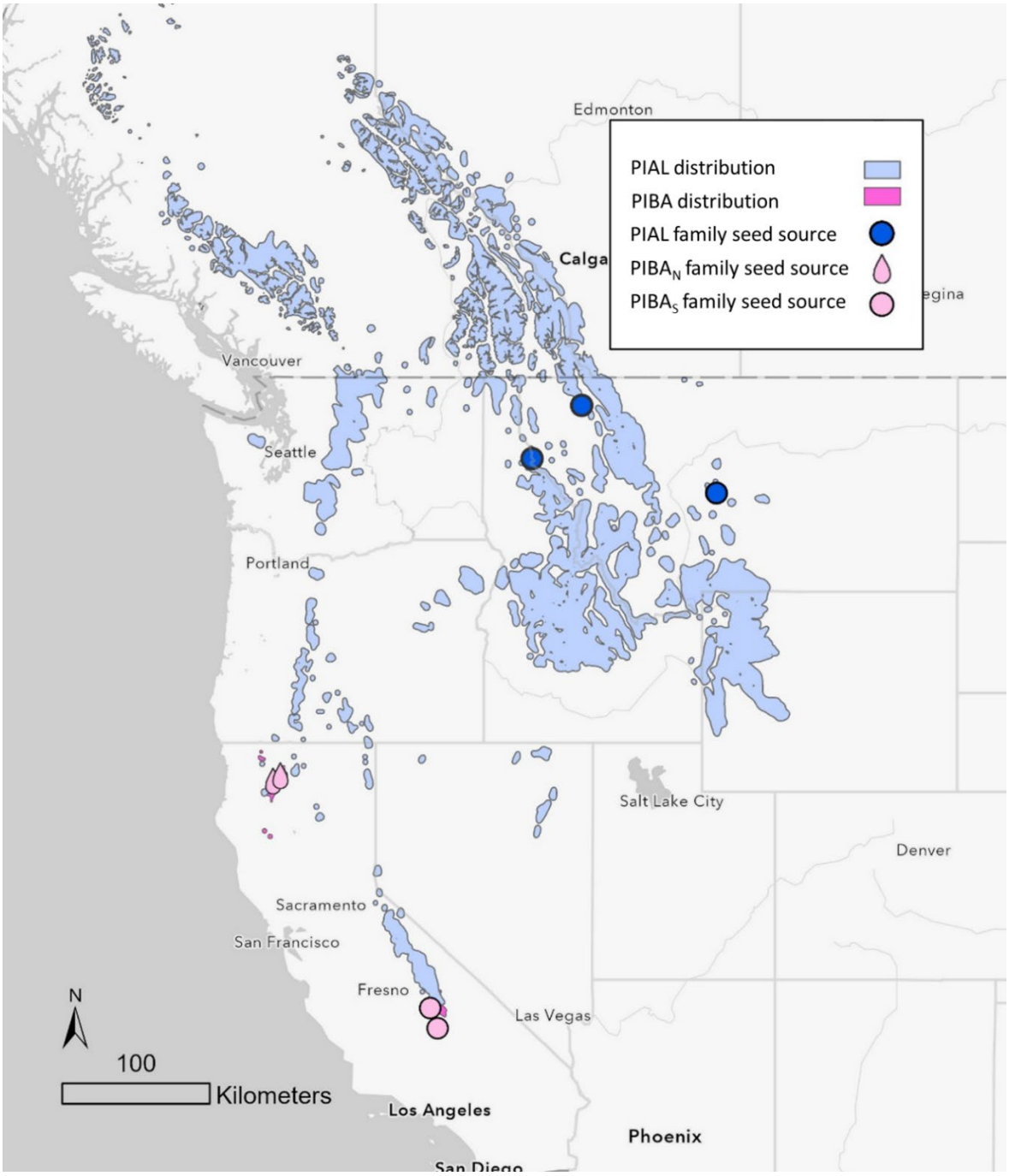

Figure 1: Species distributions and family seed source locations for whitebark pine (PIAL, blue) and foxtail pine (PIBA, pink).

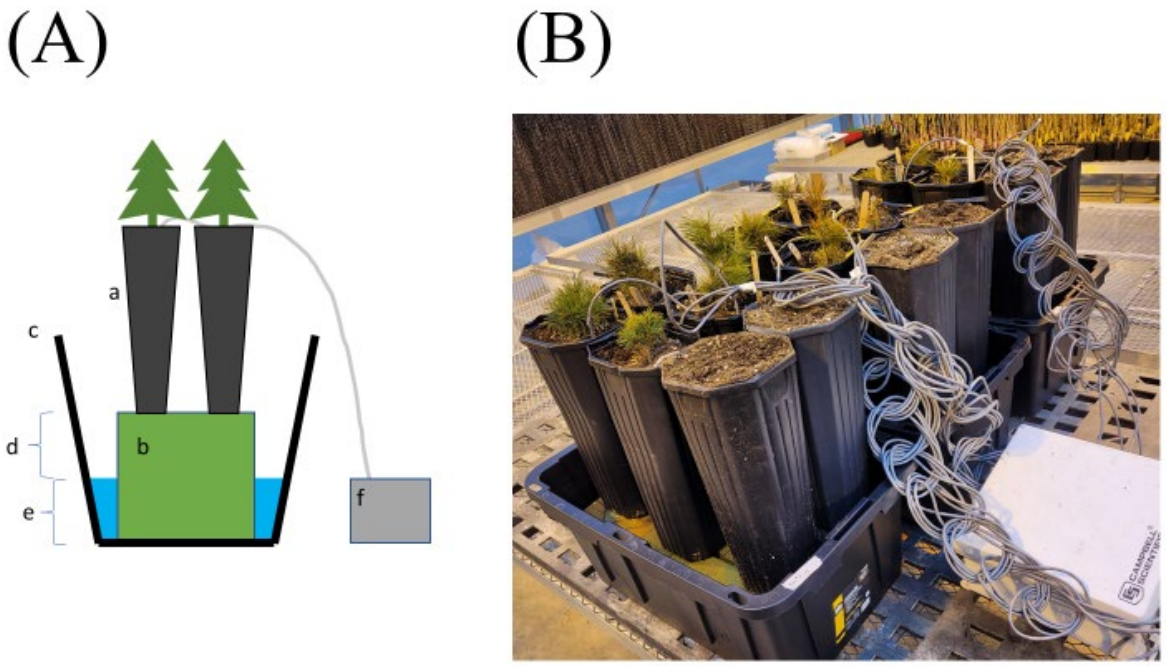

Figure 2: Diagram (A) and photo (B) of drought treatment method. Pots of juvenile trees (a) are on top of floral foam blocks (b) that draw up water from the bottom of the bin (c) to the pots. (d) is the distance between the top of the foam block and the surface of the water level, (e) is the distance between the bottom of the bin to the surface of the water level, and (f) is the soil moisture sensor.

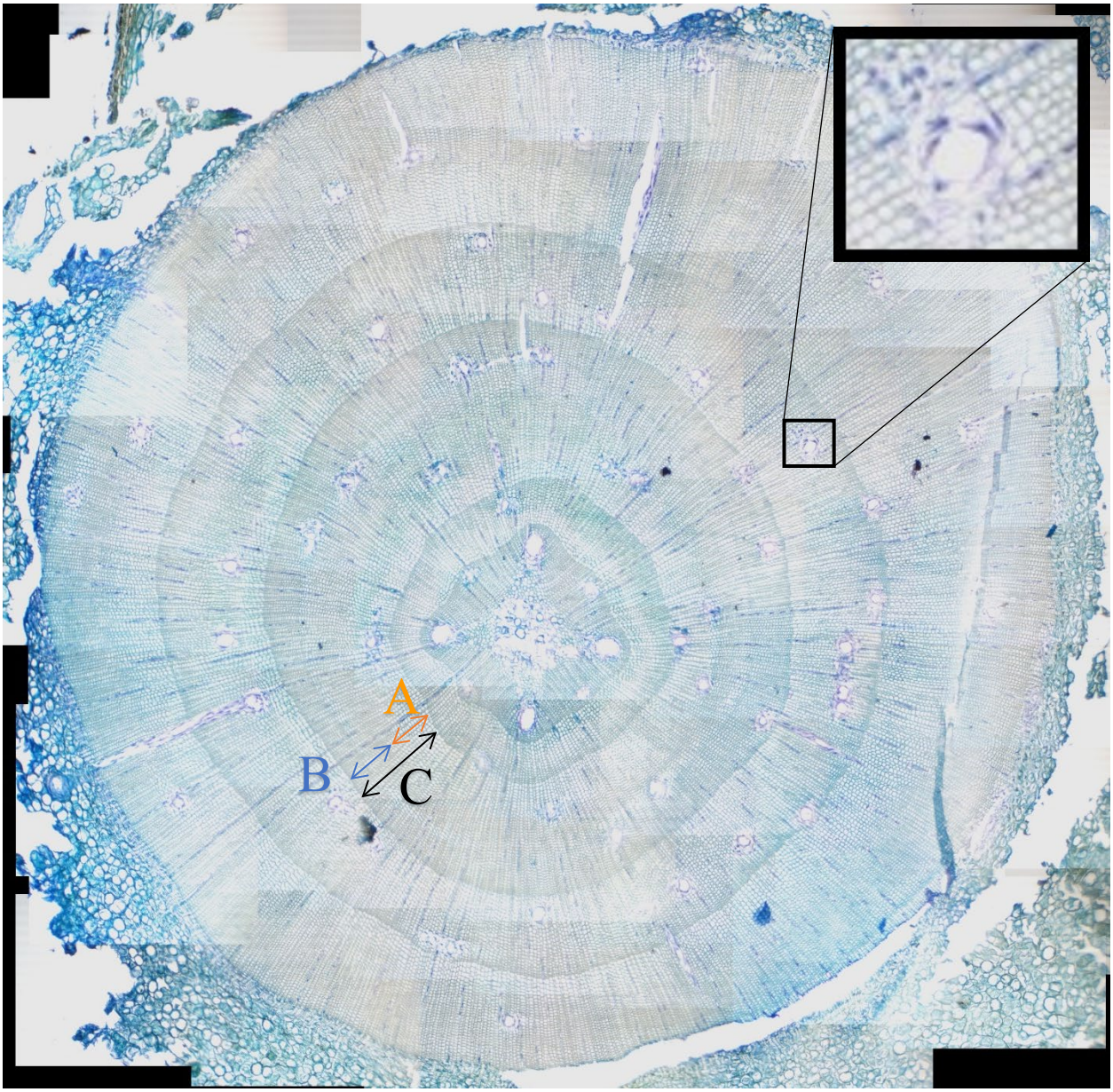

Figure 3: Example of a cross-sectional image of whitebark pine stem xylem composed of stitched images each taken at 100x magnification. The black box shows an example of a resin duct. The lines labeled A, B, and C represent the earlywood (EW) width, latewood (LW) width, and annual ring width (EW+LW), respectively for the second-year growth ring.

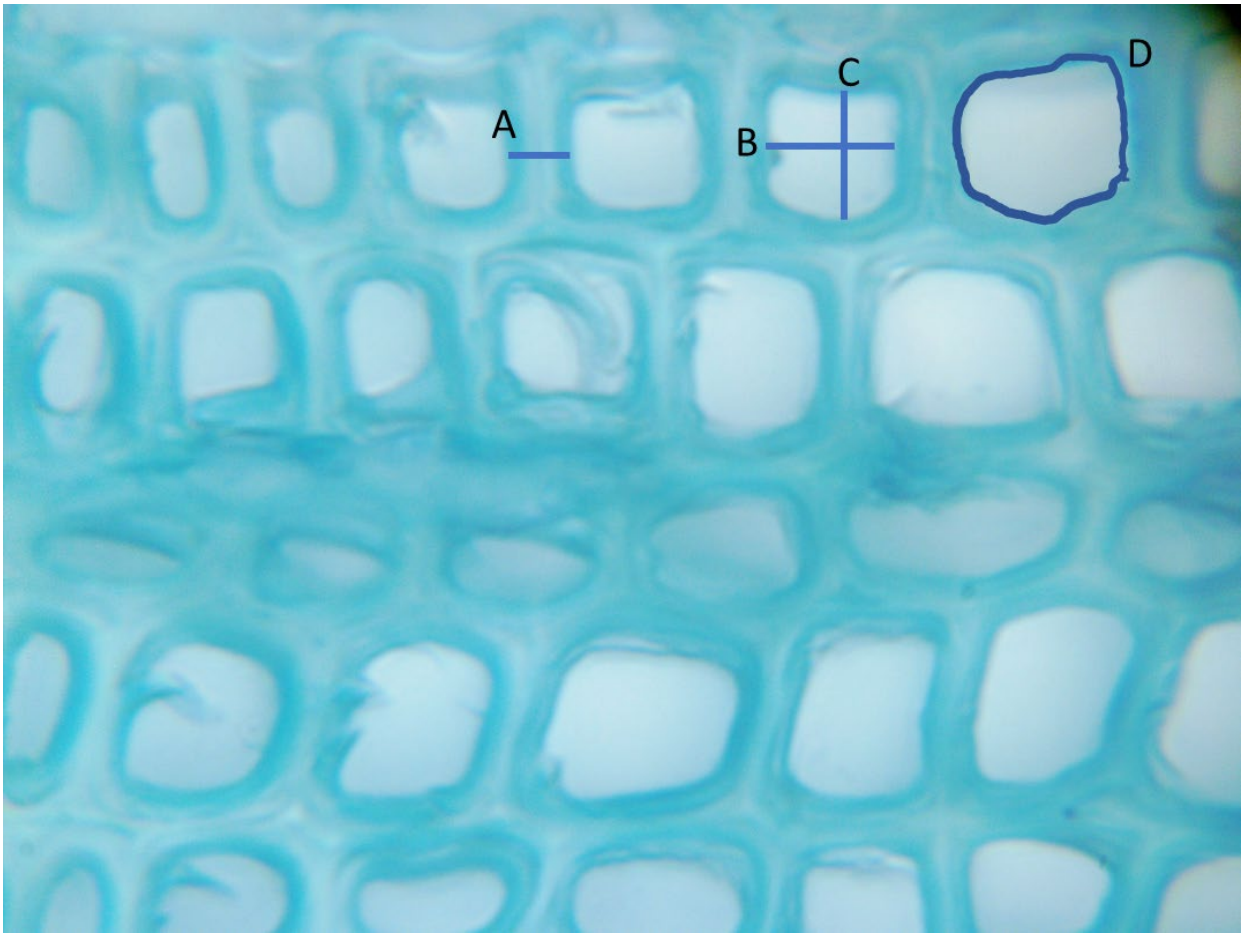

Figure 4: Image of whitebark pine xylem (1000x magnification). A is a double cell wall used to determine cell wall thickness. B and C are the major and minor axes, respectively of the assumed "ellipse" created by the lumen area (D) used to calculate potential hydraulic conductivity (K_p).

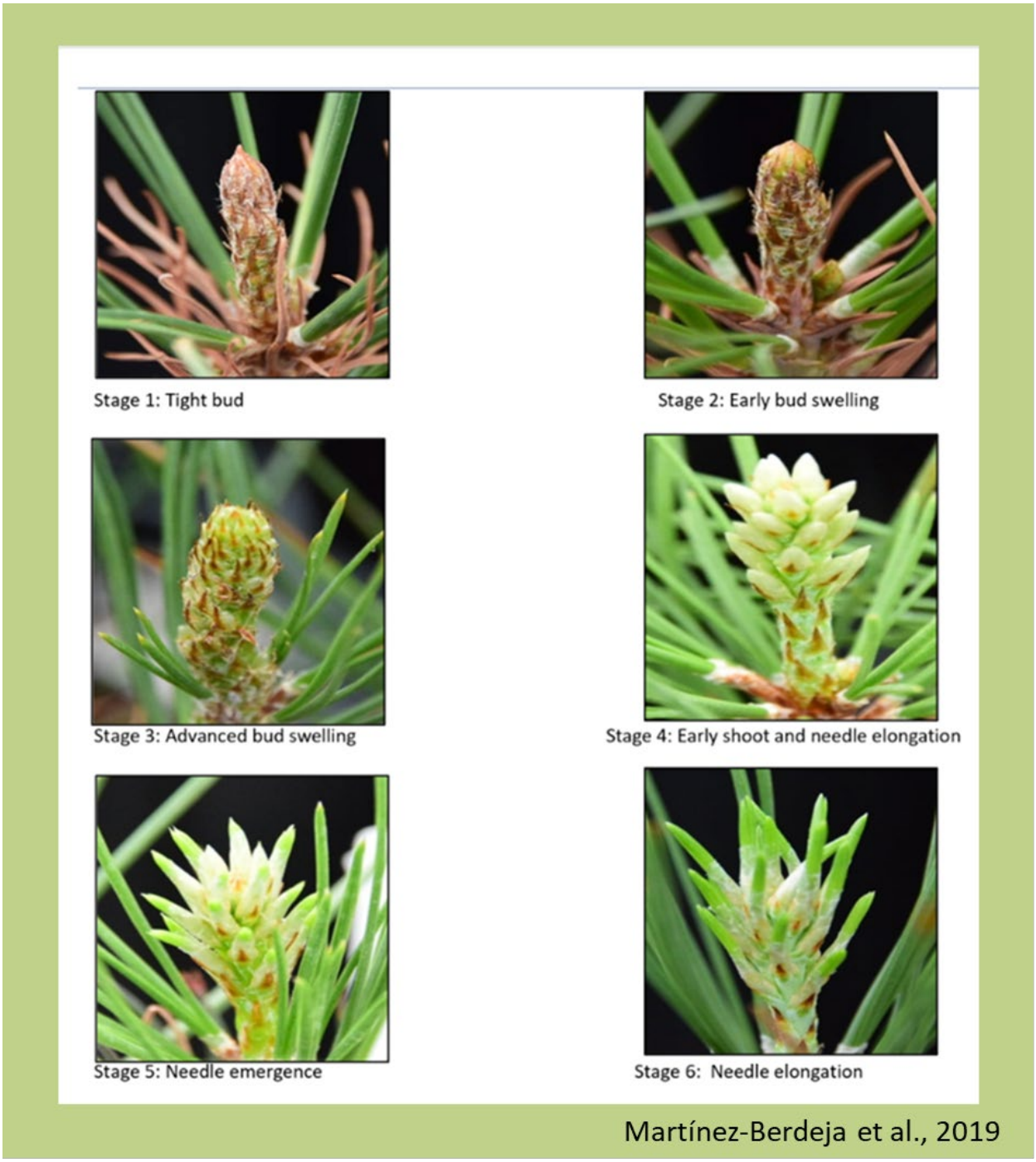

Figure 5: Six budburst stages from Martinez-Berdeja et al. 2019 used to determine budburst phenology traits.

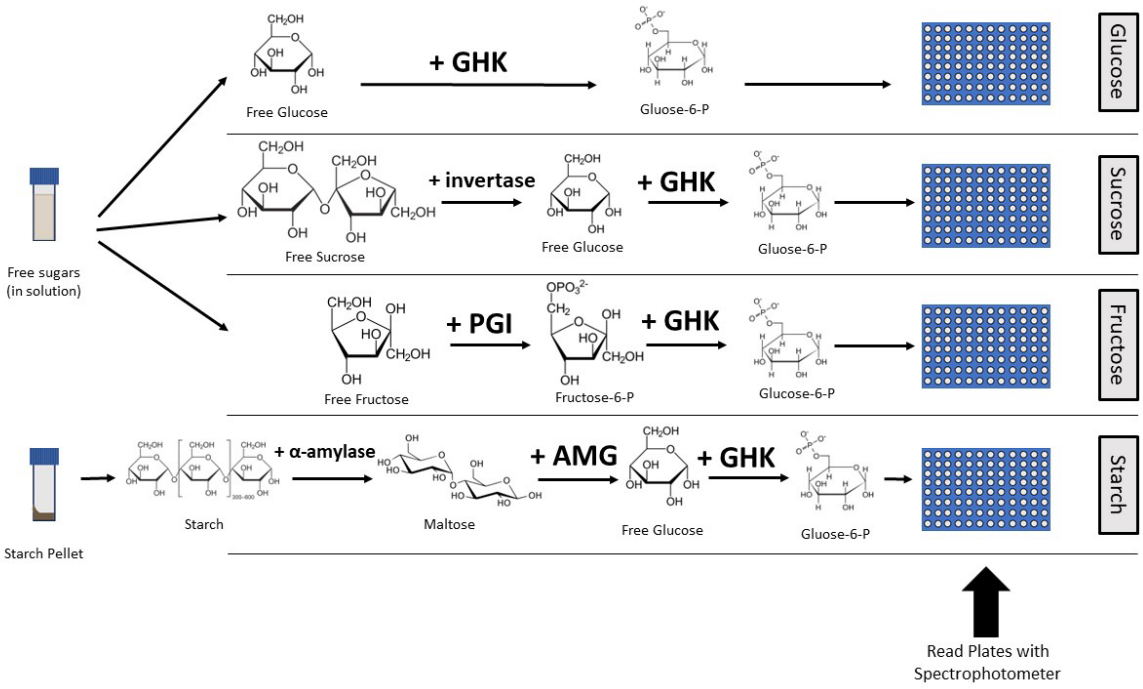

Figure 6: Diagram of the chemical reactions used to determine non-structural carbohydrate (NSC) concentrations of glucose, sucrose, fructose, and starch. GHK is glucose assay reagent, PGI is phosphoglucose isomerase, and AMG is amyloglucosidase.

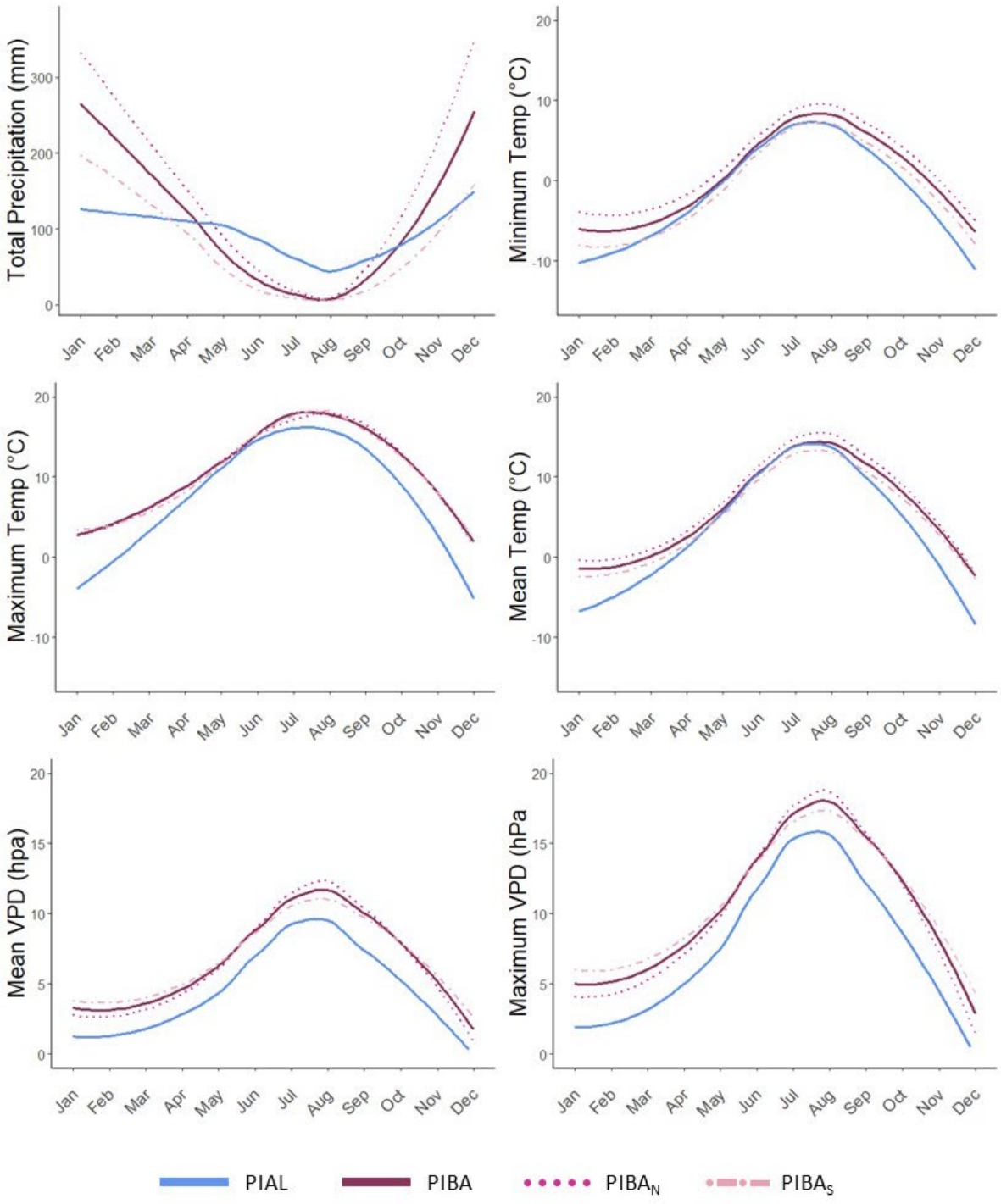

Figure 7: Annual climate variables for PIAL, PIBA, PIBA$_N$, and PIBA$_S$. Solid lines represent averages across family seed sources for PIAL (Burke, Big Mountain, Jefferson), and PIBA (267, 296, 314, 330). Dotted and dashed lines represent averages across families for PIBA$_N$ (267, 330) and PIBA$_S$ (296, 314).

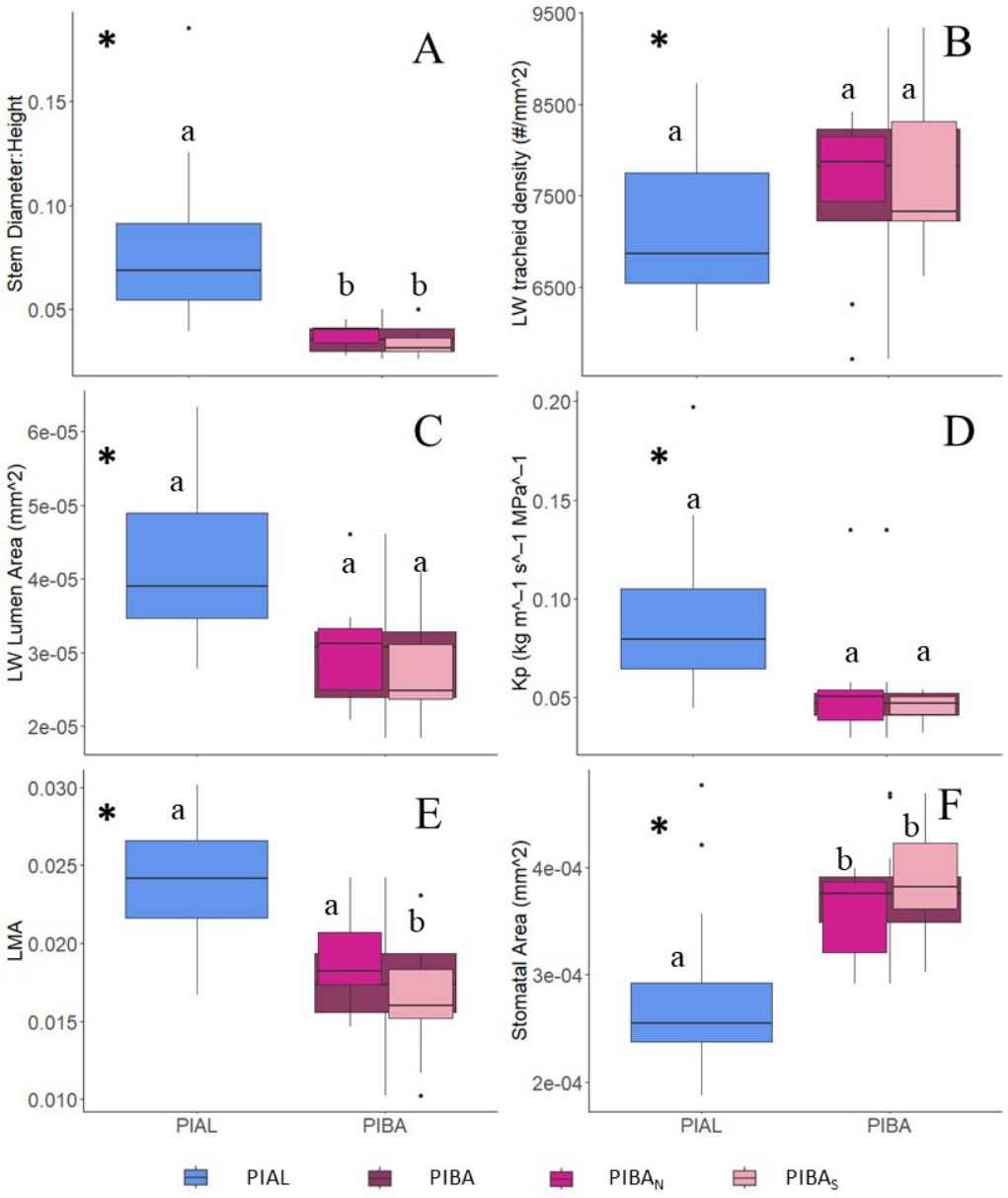

Figure 8: Boxplots of key traits of PIAL, PIBA, $PIBA_N$, and $PIBA_S$. Top and bottom lines represent first and fourth quartiles and boxes represent the second and third quartiles split by the median line. Asterisks represent significant differences between species, a, b, and c represent significant differences between PIAL and $PIBA_N$, PIAL and $PIBA_S$, and $PIBA_N$ and $PIBA_S$, respectively ($p \leq 0.05$). A is Stem Diameter:Stem Height (Stem Diameter:Height), B is Latewood (LW) tracheid density, C is Latewood (LW) Lumen Area, D is potential hydraulic conductivity (K_p), E is leaf mass per area (LMA), and F is stomatal aperture area (Stomatal Area).

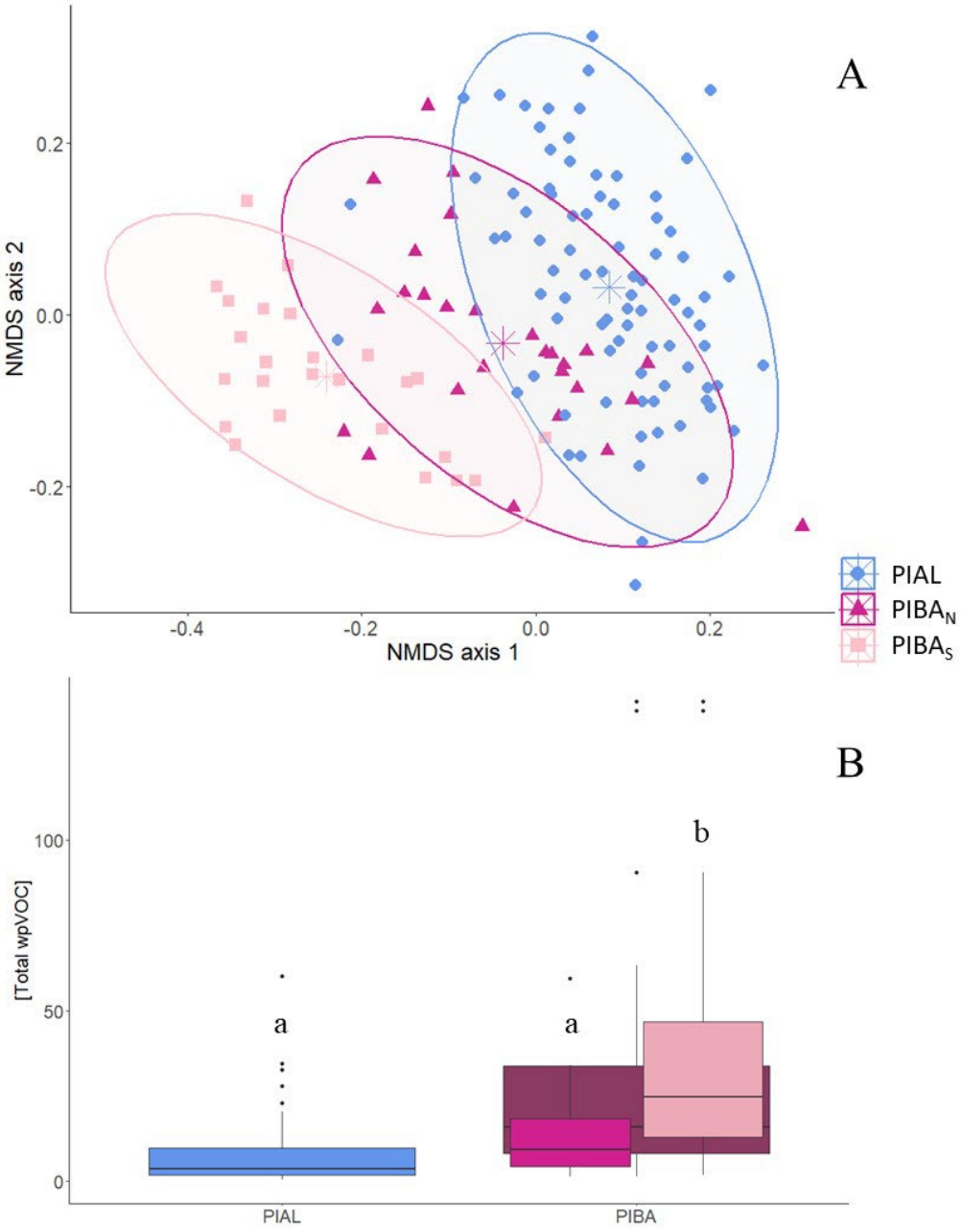

Figure 9: Nonmetric multidimensional scaling (NMDS) plot of whole plant VOCs (wpVOCs) of PIAL, PIBA$_N$, and PIBA$_S$. Central stars are the centroids for each group calculated as the average across the x- and y-axes for each group. Ellipses represent bivariate confidence intervals assuming t-distribution. Boxplots of total wpVOC concentrations for PIAL, PIBA, PIBA$_N$, and PIBA$_S$, where top and bottom lines represent first and fourth quartiles and boxes represent the second and third quartiles split by the median line. Asterisks represent significant differences between species, a, b, and c represent significant differences between PIAL and PIBA$_N$, PIAL and PIBA$_S$, and PIBA$_N$ and PIBA$_S$, respectively ($p \leq 0.05$).

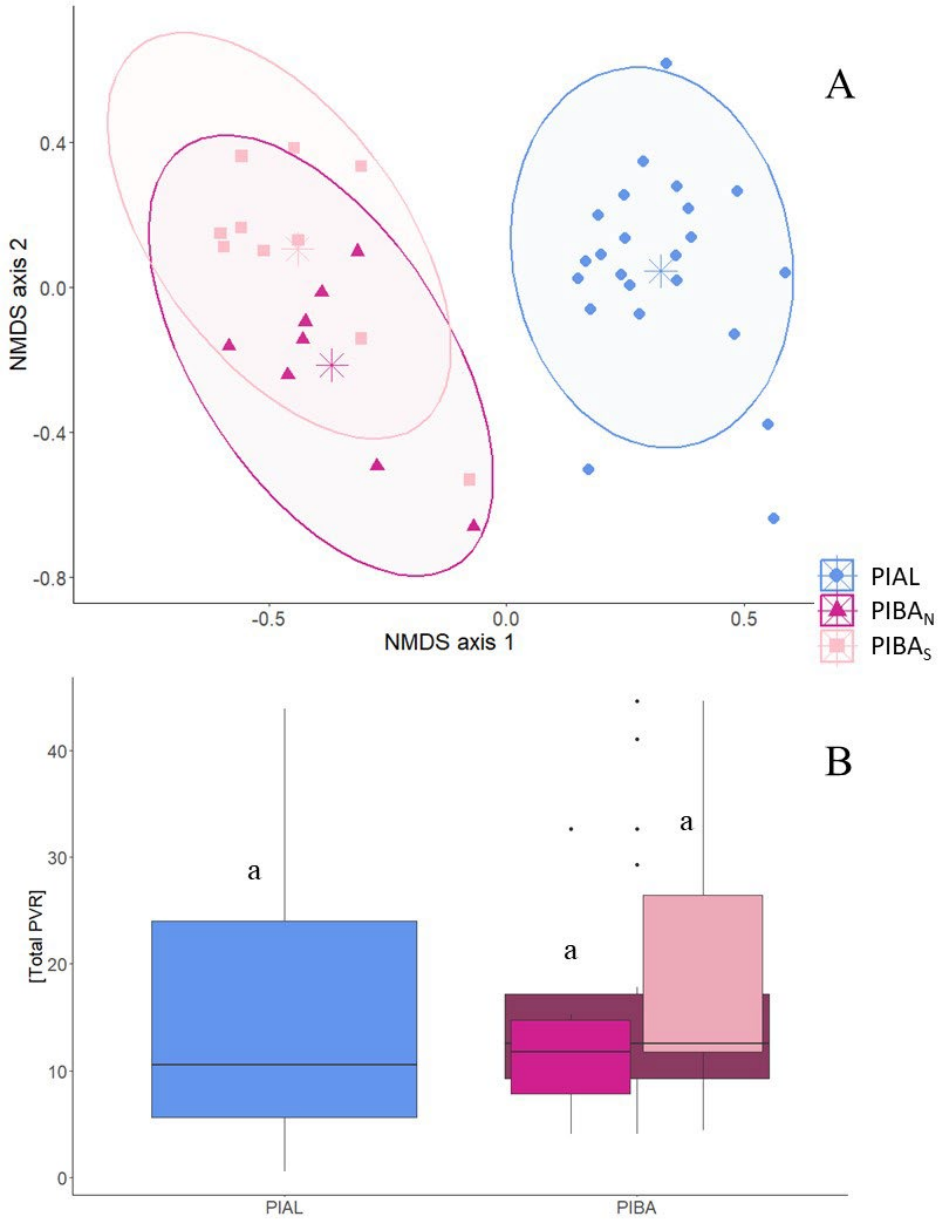

Figure 10: Nonmetric multidimensional scaling (NMDS) plot of phloem volatile resin (PVR) compounds of PIAL, PIBA$_N$, and PIBA$_S$. Central stars are the centroids for each group calculated as the average across the x- and y-axes for each group. Ellipses represent bivariate confidence intervals assuming t-distribution. Boxplots of total PVR concentrations for PIAL, PIBA, PIBA$_N$, and PIBA$_S$, where top and bottom lines represent first and fourth quartiles and boxes represent the second and third quartiles split by the median line. Asterisks represent significant differences between species, a, b, and c represent significant differences between PIAL and PIBA$_N$, PIAL and PIBA$_S$, and PIBA$_N$ and PIBA$_S$, respectively ($p \leq 0.05$).

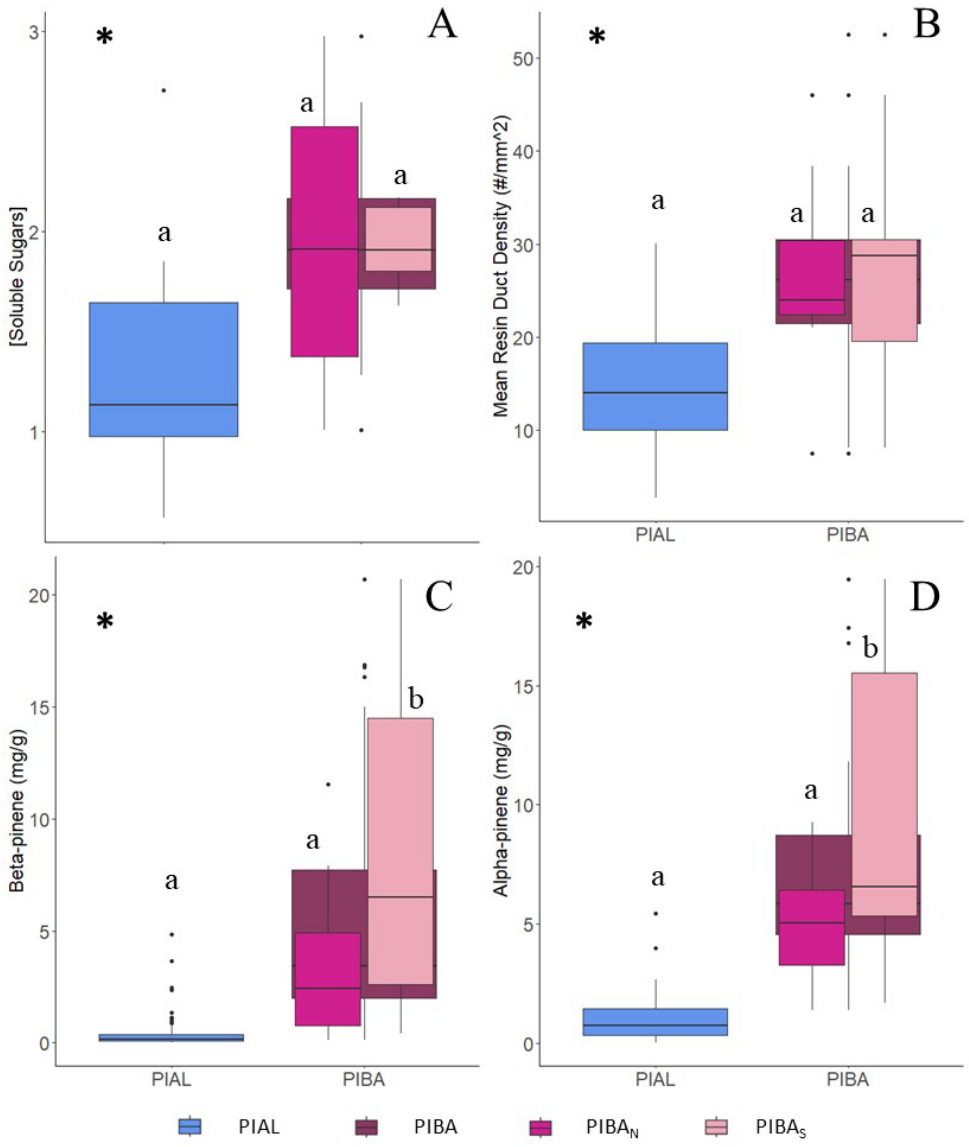

Figure 11: Boxplots of key traits of PIAL, PIBA, $PIBA_N$, and $PIBA_S$. Top and bottom lines represent first and fourth quartiles, boxes represent the second and third quartiles split by the median line. Asterisks represent significant differences between species and letters indicate significant differences between PIAL, $PIBA_N$, and $PIBA_S$ ($p \leq 0.05$). Beta-pinene is for whole plant volatile organic compounds (wpVOCs), and Alpha-pinene is for phloem volatile resin (PVR). A is the concentration of needle soluble sugars ([Soluble Sugars]), B is mean resin duct density, C is β-pinene concentrations for whole plant VOCs, and D is α-pinene concentrations for phloem volatile resin.

REFERENCES CITED

Aasamaa, K., Sõber, A., & Rahi, M. (2001). Leaf anatomical characteristics associated with shoot hydraulic conductance, stomatal conductance and stomatal sensitivity to changes of leaf water status in temperate deciduous trees. *Functional Plant Biology*, *28*(8), 765. https://doi.org/10.1071/PP00157

Adhikari, P., Shin, M.-S., Ja-Young, J., Kim, H. W., Hong, S., & Seo, C. (2018). Potential impact of climate change on the species richness of subalpine plant species in the mountain national parks of South Korea. *Journal of Ecology and Environment*, *42*, 1–10. https://doi.org/10.1186/s41610-018-0095-y

Badger, A. M., Bjarke, N., Molotch, N. P., & Livneh, B. (2021). The sensitivity of runoff generation to spatial snowpack uniformity in an alpine watershed: Green Lakes Valley, Niwot Ridge Long-Term Ecological Research station. *Hydrological Processes*, *35*(9), e14331. https://doi.org/10.1002/hyp.14331

Baumeister, D., & Callaway, R. M. (2006). Facilitation by Pinus Flexilis During Succession: A Hierarchy of Mechanisms Benefits Other Plant Species. *Ecology*, *87*(7), 1816–1830. https://doi.org/10.1890/0012-9658(2006)87[1816:FBPFDS]2.0.CO;2

Bentz, B. J., Hansen, E. M., Davenport, M., & Soderberg, D. (2022). Complexities in predicting mountain pine beetle and spruce beetle response to climate change. In *Bark Beetle Management, Ecology, and Climate Change* (pp. 31–54). Elsevier. https://doi.org/10.1016/B978-0-12-822145-7.00013-1

Bentz, B. J., Hood, S. A., Hansen, M., Vandygriff, J., & Mock, K. E. (2016a). Defense traits in the long-lived Great Basin bristlecone pine and resistance to the native herbivore mountain pine beetle. *New Phytologist. Doi: 10.1111/Nph.14191.* https://doi.org/10.1111/nph.14191

Bentz, B. J., Hood, S. A., Hansen, M., Vandygriff, J., & Mock, K. E. (2016b). Defense traits in the long-lived Great Basin bristlecone pine and resistance to the native herbivore mountain pine beetle. *New Phytologist. Doi: 10.1111/Nph.14191.* https://doi.org/10.1111/nph.14191

Bertolino, L. T., Caine, R. S., & Gray, J. E. (2019). Impact of Stomatal Density and Morphology on Water-Use Efficiency in a Changing World. *Frontiers in Plant Science*, *10*, 225. https://doi.org/10.3389/fpls.2019.00225

Brodribb, T. J., McAdam, S. A., & Carins Murphy, M. R. (2017). Xylem and stomata, coordinated through time and space. *Plant, Cell & Environment*, *40*(6), 872–880. https://doi.org/10.1111/pce.12817

Bryant, J. P., Chapin, F. S., & Klein, D. R. (1983). Carbon/Nutrient Balance of Boreal Plants in Relation to Vertebrate Herbivory. *Oikos*, *40*(3), 357–368. https://doi.org/10.2307/3544308

Burkle, L., & Runyon, J. (2017). The Smell of Environmental Change: Using Floral Scent to Explain Shifts in Pollinator Attraction. *Applications in Plant Sciences*, *5*, 1600123. https://doi.org/10.3732/apps.1600123

Campbell, E. M., Keane, R. E., Larson, E. R., Murray, M. P., Schoettle, A. W., & Wong, C. (2011). Disturbance Ecology of High-Elevation Five-Needle Pine Ecosystems in Western North America. In R. E. Keane, D. F. Tomback, M. P. Murray, & C. M. Smith (Eds.), *FUTURE OF HIGH-ELEVATION, FIVE-NEEDLE WHITE PINES IN WESTERN NORTH AMERICA: PROCEEDINGS OF THE HIGH FIVE SYMPOSIUM, 2010* (Vol. 63, pp. 154–163). Us Dept Agr, Forest Serv Rocky Mt Forest & Range Exptl Stn. https://www.webofscience.com/wos/alldb/full-record/WOS:000392553300028

de Villemereuil, P., Gaggiotti, O. E., Mouterde, M., & Till-Bottraud, I. (2016). Common garden experiments in the genomic era: New perspectives and opportunities. *Heredity*, *116*(3), Article 3. https://doi.org/10.1038/hdy.2015.93

Deslauriers, A., Fournier, M.-P., Carteni, F., & Mackay, J. (2019). Phenological shifts in conifer species stressed by spruce budworm defoliation. *TREE PHYSIOLOGY*, *39*(4), 590–605. https://doi.org/10.1093/treephys/tpy135

Domec, J., & Gartner, B. L. (2002). How do water transport and water storage differ in coniferous earlywood and latewood? *Journal of Experimental Botany*, *53*(379), 2369–2379. https://doi.org/10.1093/jxb/erf100

Drake, P. L., Froend, R. H., & Franks, P. J. (2013). Smaller, faster stomata: Scaling of stomatal size, rate of response, and stomatal conductance. *Journal of Experimental Botany*, *64*(2), 495–505. https://doi.org/10.1093/jxb/ers347

Duan, H., Huang, G., Zhou, S., & Tissue, D. T. (2018). Dry mass production, allocation patterns and water use efficiency of two conifers with different water use strategies under elevated [CO_2], warming and drought conditions. *EUROPEAN JOURNAL OF FOREST RESEARCH*, *137*(5), 605–618. https://doi.org/10.1007/s10342-018-1128-x

Dudney, J. C., Nesmith, J. C. B., Cahill, M. C., Cribbs, J. E., Duriscoe, D. M., Das, A. J., Stephenson, N. L., & Battles, J. J. (2020). Compounding effects of white pine blister rust, mountain pine beetle, and fire threaten four white pine species. *ECOSPHERE*, *11*(10), e03263. https://doi.org/10.1002/ecs2.3263

Dullinger, S., Dirnböck, T., & Grabherr, G. (2004a). Modelling climate change-driven treeline shifts: Relative effects of temperature increase, dispersal and invasibility. *Journal of Ecology*, *92*(2), 241–252. https://doi.org/10.1111/j.0022-0477.2004.00872.x

Dullinger, S., Dirnböck, T., & Grabherr, G. (2004b). Modelling climate change-driven treeline shifts: Relative effects of temperature increase, dispersal and invasibility. *Journal of Ecology*, *92*(2), 241–252. https://doi.org/10.1111/j.0022-0477.2004.00872.x

Eckert, A. J., Tearse, B. R., & Hall, B. D. (2008). A phylogeographical analysis of the range disjunction for foxtail pine (Pinus balfouriana, Pinaceae): The role of Pleistocene glaciation. *Molecular Ecology*.

El Omari, B. (2022). Accumulation versus storage of total non-structural carbohydrates in woody plants. *Trees*, *36*(3), 869–881. https://doi.org/10.1007/s00468-021-02240-6

Erbilgin, N., Zanganeh, L., Klutsch, J. G., Chen, S. hsuan, Zhao, S., Ishangulyyeva, G., Burr, S. J., Gaylord, M., Hofstetter, R., Keefover-Ring, K., Raffa, K. F., & Kolb, T. (2021). Combined drought and bark beetle attacks deplete non-structural carbohydrates and promote death of mature pine trees. *Plant Cell and Environment*, *44*(12), 3636–3651. https://doi.org/10.1111/pce.14197

Farnes, P. E. (1989). Snotel and snow course data: Describing the hydrology of whitebark pine ecosystems. *Symposium on Whitebark Pine Ecosystems*.

Felicetti, L. A., Schwartz, C. C., Rye, R. O., Haroldson, M. A., Gunther, K. A., Phillips, D. L., & Robbins, C. T. (2003). Use of sulfur and nitrogen stable isotopes to determine the importance of whitebark pine nuts to Yellowstone grizzly bears. *Canadian Journal of Zoology*, *81*(5), 763–770. https://doi.org/10.1139/z03-054

Fiedler, C. E., & McKinney, S. T. (2014). Forest Structure, Health, and Mortality in Two Rocky Mountain Whitebark Pine Ecosystems: Implications for Restoration. *Natural Areas Journal*, *34*(3), 290–299. https://doi.org/10.3375/043.034.0305

Fryer, J. L. (2004). *Pinus balfouriana*. https://www.fs.usda.gov/database/feis/plants/tree/pinbal/all.html

Fu, X., Meinzer, F. C., Woodruff, D. R., Liu, Y.-Y., Smith, D. D., McCulloh, K. A., & Howard, A. R. (2019). Coordination and trade-offs between leaf and stem hydraulic traits and stomatal regulation along a spectrum of isohydry to anisohydry. *Plant, Cell & Environment*, *42*(7), 2245–2258. https://doi.org/10.1111/pce.13543

Gibson, K., Skov, K., Kegley, S., Jorgense, C., Smith, S., & Witcosky, J. (2008). *Mountain Pine Beetle Impacts in High-Elevation Five-Needle Pines: Current Trends and Challenges*.

Goeking, S. A., & Windmuller-Campione, M. A. (2021). Comparative species assessments of five-needle pines throughout the western United States. *Forest Ecology and Management*, *496*, 119438. https://doi.org/10.1016/j.foreco.2021.119438

Government of Canada. (2017). *Recovery Strategy for the Whitebark Pine (Pinus albicaulis) in Canada*. Species at Risk Act.

Group), A. F. (IUCN S. C. S. (2011). IUCN Red List of Threatened Species: Pinus balfouriana. *IUCN Red List of Threatened Species*. https://www.iucnredlist.org/en

Guérin, M., Martin-Benito, D., Arx, G., Andreu-Hayles, L., Griffin, K. L., Hamdan, R., McDowell, N. G., Muscarella, R., Pockman, W., & Gentine, P. (2018). Interannual variations in needle and sapwood traits of *Pinus edulis* branches under an experimental drought. *Ecology and Evolution*, *8*(3), 1655–1672. https://doi.org/10.1002/ece3.3743

Hacke, U. G., Sperry, J. S., Pockman, W. T., Davis, S. D., & McCulloh, K. A. (2001). Trends in wood density and structure are linked to prevention of xylem implosion by negative pressure. *Oecologia*, *126*(4), 457–461. https://doi.org/10.1007/s004420100628

Hankin, L. E., & Bisbing, S. M. (2021). Let it snow? Spring snowpack and microsite characterize the regeneration niche of high-elevation pines. *Journal of Biogeography*, *48*(8), 2068–2084. https://doi.org/10.1111/jbi.14136

Hansen, A. J., East, A., Keane, R. E., Lavin, M., Legg, K., Holden, Z., Toney, C., & Alongi, F. (2021). Is whitebark pine less sensitive to climate warming when climate tolerances of juveniles are considered? *Forest Ecology and Management. 493: 19221.*, *493*, 19221. https://doi.org/10.1016/j.foreco.2021.119221

Hartmann, H., & Trumbore, S. (2016). Understanding the roles of nonstructural carbohydrates in forest trees – from what we can measure to what we want to know. *New Phytologist*, *211*(2), 386–403. https://doi.org/10.1111/nph.13955

Herms, D. A., & Mattson, W. J. (1992). The Dilemma of Plants: To Grow or Defend. *The Quarterly Review of Biology*, *67*(3), 283–335. https://doi.org/10.1086/417659

Holland, N., & Richardson, A. D. (2009). Stomatal Length Correlates with Elevation of Growth in Four Temperate Species †. *Journal of Sustainable Forestry*, *28*(1–2), 63–73. https://doi.org/10.1080/10549810802626142

Hood, S. M., Reed, C. C., & Kane, J. M. (2020). Axial resin duct quantification in tree rings: A functional defense trait. *MethodsX*, *7*, 101035. https://doi.org/10.1016/j.mex.2020.101035

Huang, J., Behrendt, T., Hammerbacher, A., Weinhold, A., Hellén, H., Reichelt, M., Wisthaler, A., Dam, N., Trumbore, S., & Hartmann, H. (2017). *See the forest for the trees: Whole-plant allocation patterns and regulatory mechanisms in Norway spruce*. 18204.

Huang, J., Hammerbacher, A., Weinhold, A., Reichelt, M., Gleixner, G., Behrendt, T., van Dam, N. M., Sala, A., Gershenzon, J., Trumbore, S., & Hartmann, H. (2019). Eyes on the future – evidence for trade-offs between growth, storage and defense in Norway spruce. *New Phytologist*, *222*(1), 144–158. https://doi.org/10.1111/nph.15522

IPCC. (2018). *Summary for Policymakers. In: Global Warming of 1.5°C. An IPCC Special Report on the impacts of global warming of 1.5°C above pre-industrial levels and related global greenhouse gas emission pathways, in the context of strengthening the global response to the threat of climate change, sustainable development, and efforts to eradicate poverty [Masson-Delmotte, V., P. Zhai, H.-O. Pörtner, D. Roberts, J. Skea, P.R.*

Shukla, A. Pirani, W. Moufouma-Okia, C. Péan, R. Pidcock, S. Connors, J.B.R. Matthews, Y. Chen, X. Zhou, M.I. Gomis, E. Lonnoy, T. Maycock, M. Tignor, and T. Waterfield (eds.)]. https://www.ipcc.ch/sr15/

Johnson, D. M., McCulloh, K. A., & Reinhardt, K. (2011). The earliest stages of tree growth: Development, physiology and impacts of microclimate—Reforestation, Nurseries and Genetics Resources. *Tree Physiology*, *4*, 65–87.

Keane, R. E., Holsinger, L. M., Mahalovich, M. F., & Tomback, D. F. (2017). *Restoring whitebark pine ecosystems in the face of climate change* (RMRS-GTR-361; p. RMRS-GTR-361). U.S. Department of Agriculture, Forest Service, Rocky Mountain Research Station. https://doi.org/10.2737/RMRS-GTR-361

Keen, R. M., Voelker, S. L., Wang, S.-Y. S., Bentz, B. J., Goulden, M. L., Dangerfield, C. R., Reed, C. C., Hood, S. M., Csank, A. Z., Dawson, T. E., Merschel, A. G., & Still, C. J. (2022). Changes in tree drought sensitivity provided early warning signals to the California drought and forest mortality event. *Global Change Biology. 28(3): 1119-1132.*, *28*, 1119. https://doi.org/10.1111/gcb.15973

Kreuzwieser, J., Meischner, M., Grün, M., Yáñez-Serrano, A. M., Fasbender, L., & Werner, C. (2021). Drought affects carbon partitioning into volatile organic compound biosynthesis in Scots pine needles. *The New Phytologist*, *232*(5), 1930–1943. https://doi.org/10.1111/nph.17736

Kueppers, L. M., Conlisk, E., Castanha, C., Moyes, A. B., Germino, M. J., de Valpine, P., Torn, M. S., & Mitton, J. B. (2017). Warming and provenance limit tree recruitment across and beyond the elevation range of subalpine forest. *Global Change Biology*, *23*(6), 2383–2395. https://doi.org/10.1111/gcb.13561

Lachenbruch, B., & McCulloh, K. A. (2014). Traits, properties, and performance: How woody plants combine hydraulic and mechanical functions in a cell, tissue, or whole plant. *The New Phytologist*, *204*(4), 747–764. https://doi.org/10.1111/nph.13035

Landguth, E. L., Holden, Z. A., Mahalovich, M. F., & Cushman, S. A. (2017). Using Landscape Genetics Simulations for Planting Blister Rust Resistant Whitebark Pine in the US Northern Rocky Mountains. *Frontiers in Genetics*, *8*. https://www.frontiersin.org/articles/10.3389/fgene.2017.00009

Landhäusser, S. M., Chow, P. S., Dickman, L. T., Furze, M. E., Kuhlman, I., Schmid, S., Wiesenbauer, J., Wild, B., Gleixner, G., Hartmann, H., Hoch, G., McDowell, N. G., Richardson, A. D., Richter, A., & Adams, H. D. (2018). Standardized protocols and procedures can precisely and accurately quantify non-structural carbohydrates. *Tree Physiology*, *38*(12), 1764–1778. https://doi.org/10.1093/treephys/tpy118

Letts, M. G., Nakonechny, K. N., Van Gaalen, K. E., & Smith, C. M. (2009). Physiological acclimation of Pinus flexilis to drought stress on contrasting slope aspects in Waterton

Lakes National Park, Alberta, Canada. *Canadian Journal of Forest Research*, *39*(3), 629–641. https://doi.org/10.1139/X08-206

Marchin, R. M., Backes, D., Ossola, A., Leishman, M. R., Tjoelker, M. G., & Ellsworth, D. S. (2022). Extreme heat increases stomatal conductance and drought-induced mortality risk in vulnerable plant species. *Global Change Biology*, *28*(3), 1133–1146. https://doi.org/10.1111/gcb.15976

Mason, C. J., Keefover-Ring, K., Villari, C., Klutsch, J. G., Cook, S., Bonello, P., Erbilgin, N., Raffa, K. F., & Townsend, P. A. (2019). Anatomical defences against bark beetles relate to degree of historical exposure between species and are allocated independently of chemical defences within trees. *Plant, Cell & Environment*, *42*(2), 633–646. https://doi.org/10.1111/pce.13449

McCulloh, K. A., Domec, J.-C., Johnson, D. M., Smith, D. D., & Meinzer, F. C. (2019). A dynamic yet vulnerable pipeline: Integration and coordination of hydraulic traits across whole plants. *Plant, Cell & Environment*, *42*(10), 2789–2807. https://doi.org/10.1111/pce.13607

McLane, S. C., & Aitken, S. N. (2012). Whitebark pine (Pinus albicaulis) assisted migration potential: Testing establishment north of the species range. *Ecological Applications*, *22*(1), 142–153. https://doi.org/10.1890/11-0329.1

Morgan, A. D., & Koskella, B. (2011). 6—Coevolution of Host and Pathogen. In M. Tibayrenc (Ed.), *Genetics and Evolution of Infectious Disease* (pp. 147–171). Elsevier. https://doi.org/10.1016/B978-0-12-384890-1.00006-6

Nesmith, J. C. B., Wright, M., Jules, E. S., & McKinney, S. T. (2019). Whitebark and Foxtail Pine in Yosemite, Sequoia, and Kings Canyon National Parks: Initial Assessment of Stand Structure and Condition. *Forests*, *10*(1), Article 1. https://doi.org/10.3390/f10010035

Neyret, M., Bentley, L. P., Oliveras, I., Marimon, B. S., Marimon-Junior, B. H., Almeida de Oliveira, E., Barbosa Passos, F., Castro Ccoscco, R., dos Santos, J., Matias Reis, S., Morandi, P. S., Rayme Paucar, G., Robles Cáceres, A., Valdez Tejeira, Y., Yllanes Choque, Y., Salinas, N., Shenkin, A., Asner, G. P., Díaz, S., … Malhi, Y. (2016). Examining variation in the leaf mass per area of dominant species across two contrasting tropical gradients in light of community assembly. *Ecology and Evolution*, *6*(16), 5674–5689. https://doi.org/10.1002/ece3.2281

Oline, D. K., Mitton, J. B., & Grant, M. C. (2000). Population and subspecific genetic differentiation in the foxtail pine (Pinus balfouriana). *Evolution; International Journal of Organic Evolution*, *54*(5), 1813–1819. https://doi.org/10.1111/j.0014-3820.2000.tb00725.x

Park, G., Lee, D., Kim, K., Batkhuu, N.-O., Tsogtbaatar, J., Zhu, J.-J., Jin, Y., Park, P., Hyun, J., & Kim, H. (2016). Morphological Characteristics and Water-Use Efficiency of Siberian Elm Trees (Ulmus pumila L.) within Arid Regions of Northeast Asia. *Forests*, *7*(12), 280. https://doi.org/10.3390/f7110280

Perez-Garcia, N., Font, X., Ferre, A., & Carreras, J. (2013). Drastic reduction in the potential habitats for alpine and subalpine vegetation in the Pyrenees due to twenty-first-century climate change. *REGIONAL ENVIRONMENTAL CHANGE*, *13*(6), 1157–1169. https://doi.org/10.1007/s10113-013-0427-5

Piyaruwan, H. I. G. S., Jayasinghe, P. K. S. C., & Leelamanie, D. a. L. (2020). Water repellency in eucalyptus and pine plantation forest soils and its relation to groundwater levels estimated with multi-temporal modeling. *JOURNAL OF HYDROLOGY AND HYDROMECHANICS*, *68*(4), 382–391. https://doi.org/10.2478/johh-2020-0030

Poorter, H., Niinemets, Ü., Poorter, L., Wright, I. J., & Villar, R. (2009). Causes and consequences of variation in leaf mass per area (LMA): A meta-analysis. *New Phytologist*, *182*(3), 565–588. https://doi.org/10.1111/j.1469-8137.2009.02830.x

PRISM Climate Group at Oregon State University. (n.d.-a). Retrieved August 29, 2023, from https://prism.oregonstate.edu/FAQ/

PRISM Climate Group at Oregon State University. (n.d.-b). Retrieved September 11, 2023, from https://prism.oregonstate.edu/normals/

Read, J., & Stokes, A. (2006). Plant biomechanics in an ecological context. *American Journal of Botany*, *93*(10), 1546–1565. https://doi.org/10.3732/ajb.93.10.1546

Reich, P. B., Walters, M. B., & Ellsworth, D. S. (1997). From tropics to tundra: Global convergence in plant functioning. *Proceedings of the National Academy of Sciences of the United States of America*, *94*(25), 13730–13734.

Reutemann, P. (2022). *Fastrandomforest-weka-package* [Java]. https://github.com/fracpete/fastrandomforest-weka-package (Original work published 2016)

Rissanen, K., Aalto, J., Gessler, A., Hölttä, T., Rigling, A., Schaub, M., & Bäck, J. (2022). Drought effects on volatile organic compound emissions from Scots pine stems. *Plant, Cell & Environment*, *45*(1), 23–40. https://doi.org/10.1111/pce.14219

Runyon, J. B., Bentz, B. J., & Qubain, C. A. (2022a). Constitutive and Induced Defenses in Long-lived Pines Do Not Trade Off but Are Influenced by Climate. *Journal of Chemical Ecology*, *48*(9), 746–760. https://doi.org/10.1007/s10886-022-01377-z

Runyon, J. B., Bentz, B. J., & Qubain, C. A. (2022b). Constitutive and Induced Defenses in Long-lived Pines Do Not Trade Off but Are Influenced by Climate. *JOURNAL OF*

CHEMICAL ECOLOGY, *48*(9–10), 746–760. https://doi.org/10.1007/s10886-022-01377-z

Runyon, J. B., Gray, C. A., & Jenkins, M. J. (2020). Volatiles of High-Elevation Five-Needle Pines: Chemical Signatures through Ratios and Insight into Insect and Pathogen Resistance. *JOURNAL OF CHEMICAL ECOLOGY*, *46*(3), 264–274. https://doi.org/10.1007/s10886-020-01150-0

Schaming, T. D., & Sutherland, C. S. (2020). Landscape- and local-scale habitat influences on occurrence and detection probability of Clark's nutcrackers: Implications for conservation. *PLoS ONE*, *15*(5), e0233726. https://doi.org/10.1371/journal.pone.0233726

Schindelin, J., Arganda-Carreras, I., Frise, E., Kaynig, V., Longair, M., Pietzsch, T., Preibisch, S., Rueden, C., Saalfeld, S., Schmid, B., Tinevez, J.-Y., White, D. J., Hartenstein, V., Eliceiri, K., Tomancak, P., & Cardona, A. (2012). Fiji: An open-source platform for biological-image analysis. *Nature Methods*, *9*(7), Article 7. https://doi.org/10.1038/nmeth.2019

Schoettle, A. W. (2004). Developing proactive management options to sustain bristlecone and limber pine ecosystems in the presence of a non-native pathogen. *In: Shepperd, Wayne D.; Eskew, Lane G., Compilers. 2004. Silviculture in Special Places: Proceedings of the National Silviculture Workshop; 2003 September 8-11; Granby, CO. Proceedings RMRS-P-34. Fort Collins, CO: U.S. Department of Agriculture, Forest Service, Rocky Mountain Research Station. p. 146-155*, *34*, 146–155.

Schoettle, A. W., Burns, K. S., McKinney, S. T., Krakowski, J., Waring, K. M., Tomback, D. F., & Davenport, M. (2022a). Integrating forest health conditions and species adaptive capacities to infer future trajectories of the high elevation five-needle white pines. *Forest Ecology and Management*, *521*, 120389. https://doi.org/10.1016/j.foreco.2022.120389

Schoettle, A. W., Burns, K. S., McKinney, S. T., Krakowski, J., Waring, K. M., Tomback, D. F., & Davenport, M. (2022b). Integrating forest health conditions and species adaptive capacities to infer future trajectories of the high elevation five-needle white pines. *Forest Ecology and Management*, *521*, 120389. https://doi.org/10.1016/j.foreco.2022.120389

Schwinning, S., Lortie, C. J., Esque, T. C., & DeFalco, L. A. (2022). What common-garden experiments tell us about climate responses in plants. *Journal of Ecology*, *110*(5), 986–996. https://doi.org/10.1111/1365-2745.13887

Shanahan, E., Irvine, K. M., Thoma, D., Wilmoth, S., Ray, A., Legg, K., & Shovic, H. (2016). Whitebark pine mortality related to white pine blister rust, mountain pine beetle outbreak, and water availability. *Ecosphere*, *7*(12), e01610. https://doi.org/10.1002/ecs2.1610

Shanahan, E., Irvine, K. M., Wilmoth, S., Legg, K., Daley, R., & Jackson, J. (2019). Monitoring five-needle pine on Bureau of Land Management lands in Wyoming summary report for 2013, 2014, 2016, 2017. *National Park Service*.

Sniezko, R. A., & Liu, J.-J. (2022). Genetic resistance to white pine blister rust, restoration options, and potential use of biotechnology. *Forest Ecology and Management*, *520*, 120168. https://doi.org/10.1016/j.foreco.2022.120168

Soderberg, D. N., Bentz, B. J., Runyon, J. B., Hood, S. M., & Mock, K. E. (2022). Chemical defense strategies, induction timing, growth, and trade-offs in *Pinus aristata* and *Pinus flexilis*. *Ecosphere*, *13*(8), e4183. https://doi.org/10.1002/ecs2.4183

Steppe, K., & Lemeur, R. (2007). Effects of ring-porous and diffuse-porous stem wood anatomy on the hydraulic parameters used in a water flow and storage model. *TREE PHYSIOLOGY*, *27*(1), 43–52. https://doi.org/10.1093/treephys/27.1.43

Sterck, F. J., Zweifel, R., Sass-Klaassen, U., & Chowdhury, Q. (2008). Persisting soil drought reduces leaf specific conductivity in Scots pine (Pinus sylvestris) and pubescent oak (Quercus pubescens). *Tree Physiology*, *28*(4), 529–536. https://doi.org/10.1093/treephys/28.4.529

Takahashi, K., & Miyajima, Y. (2008). Relationships between leaf life span, leaf mass per area, and leaf nitrogen cause different altitudinal changes in leaf δ13C between deciduous and evergreen species. *Botany*, *86*(11), 1233–1241. https://doi.org/10.1139/B08-093

Thoma, D. P., Shanahan, E. K., & Irvine, K. M. (2019). Climatic Correlates of White Pine Blister Rust Infection in Whitebark Pine in the Greater Yellowstone Ecosystem. *Forests*, *10*(8), Article 8. https://doi.org/10.3390/f10080666

Togashi, H. F., Prentice, I. C., Evans, B. J., Forrester, D. I., Drake, P., Feikema, P., Brooksbank, K., Eamus, D., & Taylor, D. (2015). Morphological and moisture availability controls of the leaf area-to-sapwood area ratio: Analysis of measurements on Australian trees. *Ecology and Evolution*, *5*(6), 1263–1270. https://doi.org/10.1002/ece3.1344

Tomback, D. F., & Achuff, P. (2010). Blister rust and western forest biodiversity: Ecology, values and outlook for white pines. *Forest Pathology*, *40*(3–4), 186–225. https://doi.org/10.1111/j.1439-0329.2010.00655.x

Tomback, D. F., Anderies, A. J., Carsey, K. S., Powell, M. L., & Mellmann-Brown, S. (2001). Delayed Seed Germination in Whitebark Pine and Regeneration Patterns Following the Yellowstone Fires. *Ecology*, *82*(9), 2587–2600. https://doi.org/10.1890/0012-9658(2001)082[2587:DSGIWP]2.0.CO;2

Tomback, D. F., Keane, R. E., Schoettle, A. W., Sniezko, R. A., Jenkins, M. B., Nelson, C. R., Bower, A. D., DeMastus, C. R., Guiberson, E., Krakowski, J., Murray, M. P., Pansing, E. R., & Shamhart, J. (2022). Tamm review: Current and recommended management practices for the restoration of whitebark pine (Pinus albicaulis Engelm.), an imperiled high-elevation Western North American forest tree. *Forest Ecology and Management*, *522*, 119929. https://doi.org/10.1016/j.foreco.2021.119929

Tuswa, N., Bugan, R. D. H., Mapeto, T., Jovanovic, N., Gush, M., Kapangaziwiri, E., Dzikiti, S., Kanyerere, T., & Xu, Y. (2019). The impacts of commercial plantation forests on groundwater recharge: A case study from George (Western Cape, South Africa). *PHYSICS AND CHEMISTRY OF THE EARTH*, *112*, 187–199. https://doi.org/10.1016/j.pce.2018.12.006

Ulrich, D. E. M., Wasteneys, C., Hoy-Skubik, S., & Alongi, F. (2023a). Functional traits underlie specialist-generalist strategies in whitebark pine and limber pine. *Forest Ecology and Management*, *542*, 121113. https://doi.org/10.1016/j.foreco.2023.121113

Ulrich, D. E. M., Wasteneys, C., Hoy-Skubik, S., & Alongi, F. (2023b). Functional traits underlie specialist-generalist strategies in whitebark pine and limber pine. *Forest Ecology and Management*, *542*, 121113. https://doi.org/10.1016/j.foreco.2023.121113

USFWS. (2022, December 15). *Endangered and Threatened Wildlife and Plants; Threatened Species Status With Section 4(d) Rule for Whitebark Pine (Pinus albicaulis)*. Federal Register. https://www.federalregister.gov/documents/2022/12/15/2022-27087/endangered-and-threatened-wildlife-and-plants-threatened-species-status-with-section-4d-rule-for

Wang, Q., Cox, M. E., Hammond, A. P., & Preda, M. (2008). Deep weathering profile and groundwater characteristics within a low-lying coastal pine plantation, southern Queensland—Relationship to water-logging and salinisation. *AUSTRALIAN FORESTRY*, *71*(2), 122–134. https://doi.org/10.1080/00049158.2008.10676279

Wright, I. J., Reich, P. B., Westoby, M., Ackerly, D. D., Baruch, Z., Bongers, F., Cavender-Bares, J., Chapin, T., Cornelissen, J. H. C., Diemer, M., Flexas, J., Garnier, E., Groom, P. K., Gulias, J., Hikosaka, K., Lamont, B. B., Lee, T., Lee, W., Lusk, C., … Villar, R. (2004). The worldwide leaf economics spectrum. *Nature*, *428*(6985), Article 6985. https://doi.org/10.1038/nature02403

Wright, I. J., & Westoby, M. (2002). Leaves at low versus high rainfall: Coordination of structure, lifespan and physiology. *New Phytologist*, *155*(3), 403–416. https://doi.org/10.1046/j.1469-8137.2002.00479.x

Wyka, S. A., Munck, I. A., Brazee, N. J., & Broders, K. D. (2018). Response of eastern white pine and associated foliar, blister rust, canker and root rot pathogens to climate change. *Forest Ecology and Management*, *423*, 18–26. https://doi.org/10.1016/j.foreco.2018.03.011

Xu, Z., & Zhou, G. (2008). Responses of leaf stomatal density to water status and its relationship with photosynthesis in a grass. *Journal of Experimental Botany*, *59*(12), 3317–3325. https://doi.org/10.1093/jxb/ern185

Yang, H., & Wang, G. (2001, January 1). *Leaf stomatal densities and distribution in triticum aestivum under drought and CO_(2) enrichmen*. Acta Phytoecological Sinica.

Yang, S., Sterck, F. J., Sass-Klaassen, U., Cornelissen, J. H. C., van Logtestijn, R. S. P., Hefting, M., Goudzwaard, L., Zuo, J., & Poorter, L. (2022). Stem Trait Spectra Underpin Multiple Functions of Temperate Tree Species. *Frontiers in Plant Science*, *13*, 769551. https://doi.org/10.3389/fpls.2022.769551

Young, D. J. N., Slaton, M. R., & Koltunov, A. (2023). Temperature is positively associated with tree mortality in California subalpine forests containing whitebark pine. *ECOSPHERE*, *14*(2), e4400. https://doi.org/10.1002/ecs2.4400

Zheng, J., Li, Y., Morris, H., Vandelook, F., & Jansen, S. (2022). Variation in Tracheid Dimensions of Conifer Xylem Reveals Evidence of Adaptation to Environmental Conditions. *Frontiers in Plant Science*, *13*, 774241. https://doi.org/10.3389/fpls.2022.774241

Zhong, M., Cerabolini, B. E. L., Castro-Díez, P., Puyravaud, J., & Cornelissen, J. H. C. (2020). Allometric co-variation of xylem and stomata across diverse woody seedlings. *Plant, Cell & Environment*, *43*(9), 2301–2310. https://doi.org/10.1111/pce.13826

APPENDICES

APPENDIX A

FIGURES

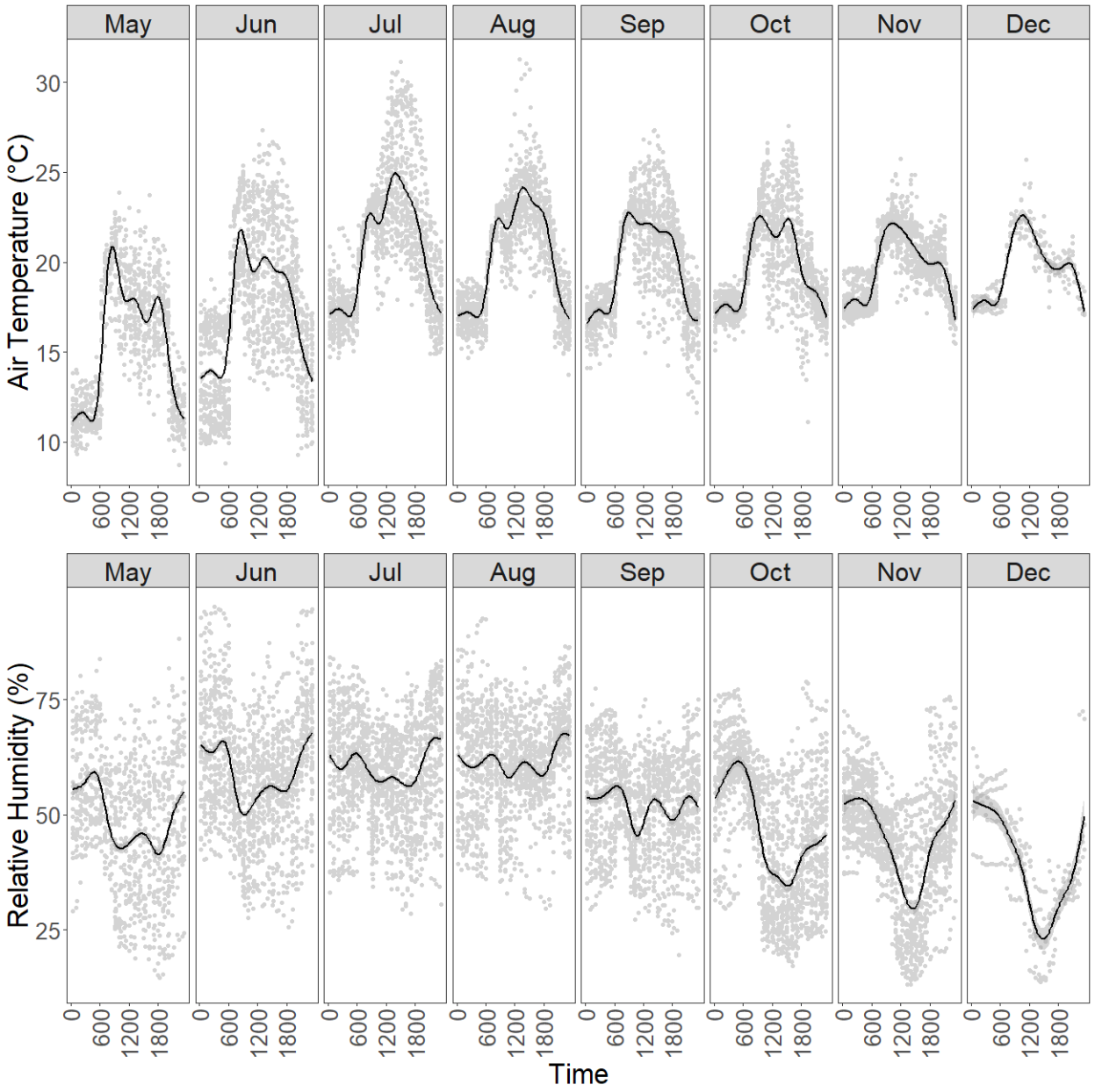

Appendix figure 1. Monthly air temperature and relative humidity in the greenhouse during study period (12 June 2022 to 9 Dec 2022).

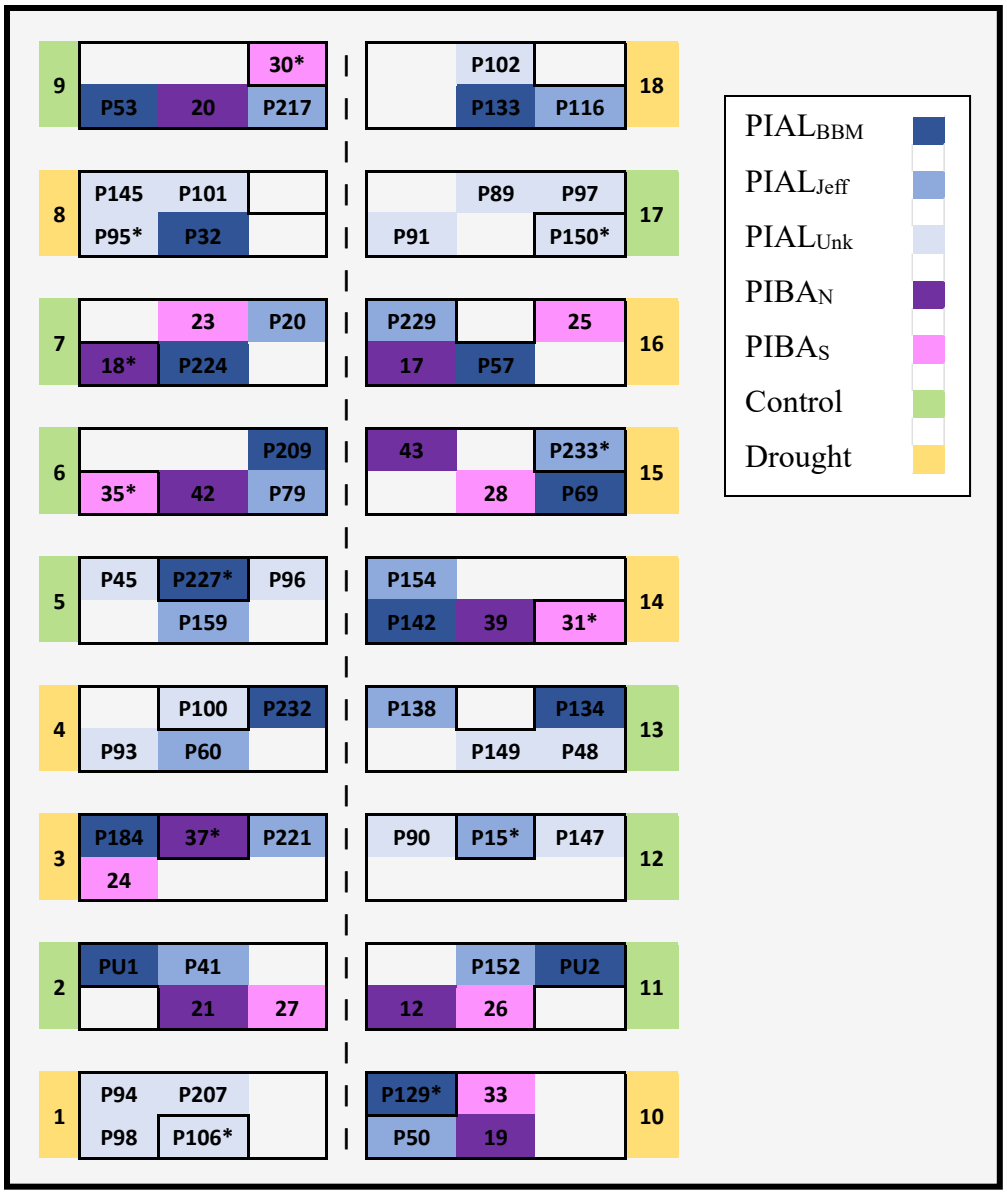

Appendix figure 2. Diagram of greenhouse experimental design. Large rectangles represent bins that contained six pots per bin. Numbers beside the bin are bin numbers. Treatment (control (green), drought (yellow)) was randomly assigned to each bin. Numbers inside the bin are individual tree identification numbers. Different colors within each bin represent different families, where PIALBBM are from Burke/Big Mountain (dark blue), PIALJeff are from Jefferson (blue), PIALUnk are from unknown family seed sources (light blue), PIBAN are from the northern PIBA population (purple), and PIBAS are from the southern PIBA population (pink). Asterisks indicate individuals that had a continuous hourly volumetric water content (VWC) sensor placed in the soil. White (blank) positions with no numbers in bins are individuals that were not used in this study.

APPENDIX B

TABLES

Appendix Table 1: Site locations where untagged juveniles may have originated from (in addition to Jefferson, Big Mountain, and Burke).

Lot id	**Latitude**	**Longitude**	**Elevation (m)**	**Location**
7694	47.74	-115.39	1962.82	Montana
7678	46.50	-111.27	2316.37	Montana
JEFFERSON 11	46.87	-110.66	2285.89	Montana
JHMR850014	43.60	-110.85	2590.67	Wyoming
WHEELERMTN14	45.50	-111.08	2519.05	Montana
BIGMTN13	48.50	-114.35	1859.19	Montana
BURKE12	47.51	-115.71	1889.67	Idaho

Appendix Table 1. Climate comparisons between PIAL, $PIBA_N$, and $PIBA_S$. Bolded p-values indicate significant differences at p-value ≤ 0.05.

		PIBA - PIAL		PIAL - $PIBA_N$		$PIBA_S$ - PIAL		$PIBA_S$ - $PIBA_N$	
	Climate Trait	estimate	p-value	estimate	p-value	estimate	p-value	estimate	p-value
Annual	Mean Precipitation	22.706	0.467	-59.118	0.081	-13.706	0.774	-72.824	**0.057**
	Average Minimum Temperature	2.125	0.187	-3.558	0.112	0.692	0.864	-2.867	0.232
	Average Temperature	2.459	**0.041**	-3.299	**0.050**	1.619	0.294	-1.679	0.324
	Average Maximum Temperature	2.794	**0.005**	-3.033	**0.032**	2.554	**0.056**	-0.479	0.833
	Average Dewpoint	-0.973	0.534	-0.642	0.874	-2.588	0.220	-3.229	0.164
	Average Minumum VPD	1.260	**0.001**	-1.342	**0.006**	1.178	**0.010**	-0.165	0.761
	Average Maximum VPD	2.915	**0.001**	-2.523	**0.014**	3.307	**0.005**	0.783	0.392
	Average VPD	2.087	**0.000**	-1.933	**0.002**	**2.242**	**0.001**	0.309	0.434
	Maximum Temperature	-0.908	0.434	-0.167	0.986	-1.983	0.249	-2.150	0.254
	Minimum Temperature	3.250	0.118	-5.100	0.066	1.400	0.673	-3.700	0.195
	Temperature Range	-4.158	**0.021**	4.933	0.066	-3.383	0.178	1.550	0.650
Growing Season (Mar-Aug)	Mean Precipitation	-31.415	**0.031**	17.271	0.086	-45.560	**0.003**	-28.289	**0.025**
	Average Minimum Temperature	0.861	0.516	-2.094	0.299	-0.372	0.949	-2.467	0.261
	Average Temperature	0.593	0.552	-1.531	0.313	-0.344	0.925	-1.875	0.254
	Average Maximum Temperature	0.332	0.670	-0.961	0.510	-0.297	0.927	-1.258	0.405
	Average Dewpoint	-1.811	0.151	0.719	0.774	-2.903	0.097	-2.183	0.239
	Average Minumum VPD	1.585	**0.008**	-1.830	**0.031**	1.341	0.081	-0.489	0.609
	Average Maximum VPD	2.501	**0.003**	-2.644	**0.025**	2.358	0.037	-0.286	0.904
	Average VPD	2.043	**0.001**	-2.237	**0.005**	1.849	**0.010**	-0.388	0.562
	Maximum Temperature	-0.908	0.434	-0.167	0.986	-1.983	0.249	-2.150	0.254
	Minimum Temperature	0.358	0.809	-1.883	0.388	-1.167	0.658	-3.050	0.186
	Temperature Range	-1.267	0.258	1.717	0.439	-0.817	0.803	0.900	0.801

Winter Season (Sep-Feb)	Mean Precipitation	76.827	0.179	-59.118	0.081	-13.706	0.774	-72.824	**0.057**
	Average Minimum Temperature	3.389	0.081	-3.558	0.112	0.692	0.864	-2.867	0.232
	Average Temperature	4.325	**0.004**	-3.299	**0.050**	1.619	0.294	-1.679	0.324
	Average Maximum Temperature	5.256	**0.000**	-3.033	**0.032**	2.554	0.056	-0.479	0.833
	Average Dewpoint	-0.135	0.945	-0.642	0.874	-2.588	0.220	-3.229	0.164
	Average Minumum VPD	0.934	**0.000**	-1.342	**0.006**	1.178	**0.010**	-0.165	0.761
	Average Maximum VPD	3.329	**0.005**	-2.523	**0.014**	3.307	**0.005**	0.783	0.392
	Average VPD	2.132	**0.003**	-1.933	**0.002**	2.242	**0.001**	0.309	0.434
	Maximum Temperature	4.450	**0.001**	-0.167	0.986	-1.983	0.249	-2.150	0.254
	Minimum Temperature	3.250	0.118	-5.100	**0.066**	1.400	0.673	-3.700	0.195
	Temperature Range	1.200	0.461	4.933	**0.066**	-3.383	0.178	1.550	0.650

Appendix table 2: Results of linear mixed effects models for all comparisons and traits in this study. Bolded p-values are significantly different contrasts at p-value ≤ 0.05.

		PIAL	$PIBA_N$	$PIBA_S$	PIBA - PIAL		$PIBA_N$ - PIAL		PIAL – $PIBA_S$		$PIBA_N$ – $PIBA_S$	
	Trait	n =	n =	n =	est.	p-val.	est.	p-val.	est.	p-val.	est.	p-val.
Morphology	Stem Diameter	62	9	8	-2.10	**0.01**	-1.93	0.08	2.30	**0.05**	0.37	0.98
	Stem height	62	8	8	32.52	**0.03**	20.11	0.55	-44.92	**0.05**	-24.81	0.57
	Stem Diameter : Stem Height	62	8	8	-0.04	**2.18E-04**	-0.04	**3.05E-03**	0.04	**2.68E-03**	2.97E-03	0.99
	Fascicle Density	59	8	8	-0.04	0.31	-0.03	0.94	0.06	0.66	0.03	0.96
	Mean Branch Diameter	59	8	8	-0.99	**0.02**	-0.94	0.16	1.03	0.14	0.09	1.00
	Mean Branch Length	59	8	8	12.77	0.17	6.42	0.83	-20.98	0.13	-14.56	0.43
	Branch Diameter : Branch Length	59	8	8	-0.04	**0.04**	-0.04	0.30	0.05	0.17	0.01	0.95
	Branch Diameter : Stem Diameter	59	8	8	0.01	0.77	0.05	0.83	0.02	0.98	0.07	0.73
	Leaf Area (Total)	28	8	10	8.60	0.84	-41.53	0.70	-55.08	0.53	-96.62	0.20
	LMA	28	9	10	-0.01	**0.01**	-0.01	0.11	0.01	**0.03**	2.81E-03	0.53
	Leaf Area : Sapwood Area	27	6	8	524.18	0.21	-15.26	1.00	-1113.91	**0.01**	-1129.18	**2.40E-03**
	STAR	28	8	10	-57.44	**0.01**	-38.00	0.20	72.58	**0.05**	34.58	0.31
	Canopy Area	59	8	8	-4367.78	**0.01**	-4205.44	**0.05**	4530.12	**0.04**	324.68	1.00
	Needle Dry Biomass	38	9	10	-0.77	0.28	-1.46	0.26	0.09	1.00	-1.37	0.43
	Stem Dry Biomass	39	9	10	-0.14	0.79	-0.31	0.96	-2.94E-03	1.00	-0.31	0.97
	Root Dry Biomass	39	9	10	-0.72	0.55	-0.76	0.95	0.65	0.97	-0.11	1.00
	Aboveground Biomass : Belowground Biomass	37	9	10	-0.71	0.15	-0.94	0.33	0.51	0.76	-0.43	0.90

Stomata	Aperture Area	50	8	8	0.00	**2.86E-03**	8.28E-05	**0.04**	-1.19E-04	**0.01**	-3.62E-05	0.64
	Guard Cell Area	50	8	8	0.00	**0.01**	1.60E-04	0.17	-3.11E-04	**0.02**	-1.51E-04	0.30
	Aperture Length	50	8	8	0.00	**2.14E-03**	3.55E-03	**0.01**	-2.40E-03	0.08	1.15E-03	0.71
	Stomata Density	50	8	8	-0.58	0.16	-0.35	0.86	0.80	0.35	0.45	0.85
	Number of Rows	50	8	8	0.38	**6.89E-04**	0.52	**0.00**	-0.25	0.07	0.27	0.10
	Number of Stomata	50	8	8	-0.33	0.10	-0.26	0.66	0.40	0.35	0.14	0.95
Xylem	Earlywood Ring Width	23	8	9	-0.09	0.07	-0.10	0.21	0.09	0.29	0.00	1.00
	Latewood Ring Width	23	8	9	-0.04	0.21	-0.06	0.35	0.04	0.59	-0.02	0.83
	EW:LW Ring Width	23	8	9	-0.17	0.63	-0.11	0.96	0.20	0.85	0.10	0.10
	Annual Ring Width	23	8	9	-0.14	0.07	-0.15	0.18	0.13	0.29	-0.03	0.95
	Resin Duct Area	23	8	9	0.00	**0.04**	-7.22E-04	**0.05**	4.17E-04	0.27	-3.06E-04	0.48
	Resin Duct Density	23	8	9	9.04	**0.05**	8.36	0.25	-9.58	0.19	-1.23	0.97
	Earlywood Lumen Area	23	8	9	-1.70E-05	0.09	-1.41E-05	0.38	1.96E-05	0.24	5.46E-06	0.88
	Latewood Lumen Area	23	8	9	-1.09E-05	**0.05**	-9.69E-06	0.21	1.19E-05	0.20	2.18E-06	0.89
	Earlywood Tracheid Density	23	8	9	9.38E-05	0.72	-2.18E-04	0.76	-3.70E-04	0.48	-5.88E-04	0.28
	Latewood Tracheid Density	23	8	9	9.25E-04	**0.03**	9.61E-04	0.11	-9.16E-04	0.15	4.52E-05	0.99
	Earlywood Cell Wall Thickness	23	8	9	1.34E-04	0.18	2.48E-04	**0.02**	-2.28E-05	0.91	2.25E-04	**0.04**
	Latewood Cell Wall Thickness	23	8	9	-2.07E-04	0.52	3.27E-05	1.00	4.14E-04	0.52	4.46E-04	0.56
	Potential Hydraulic Conductivity (Kp)	23	8	9	-4.52E-08	**0.05**	-3.95E-08	0.28	5.21E-08	0.16	1.26E-08	0.87
	Vessel Implosion Resistance (VIR)	23	8	9	0.09	0.20	0.11	0.40	-0.08	0.61	0.03	0.93

Budburst	Days between Stage 1 and Stage 2	48	8	10	41.46	**0.04**	64.76	**0.01**	-21.86	0.42	42.90	0.10
	Days between Stage 1 and Stage 3	41	5	10	53.32	**0.02**	39.22	0.44	-60.37	0.07	-21.16	0.88
	Days between Stage 1 and Stage 4	26	6	5	17.17	0.07	19.03	0.30	-14.46	0.50	4.56	0.98
	Days between Stage 1 and Stage 5	5	6	4	14.40	0.50	16.36	0.92	-10.03	0.98	6.33	1.00
	Days between Stage 1 and Stage 6	6	5	4	35.27	**0.02**	30.60	0.23	-40.39	0.12	-9.78	0.90
Physiology	Photosynthetic Rate (A)	15	6	9	-1.10	0.44	0.23	1.00	2.55	0.35	2.79	0.36
	Stomatal Conductance	15	6	9	-0.01	0.56	1.93E-03	1.00	0.01	0.76	0.02	0.74
	Water Potential Difference (Midday - Predawn)	15	6	9	-0.02	0.74	-0.08	0.66	-0.03	1.00	-0.11	0.46
	Midday Water Potential	15	6	9	0.03	0.64	-0.05	1.00	-0.09	0.72	-0.14	0.39
	Pre-Dawn Water Potential	15	6	9	0.02	0.71	-0.01	1.00	-0.04	1.00	-0.05	1.00
	Leaf Temperature	15	6	9	0.43	0.26	0.30	1.00	-0.52	0.91	-0.22	1.00
Whole Plant VOCs	β-Pinene	40	9	9	5.59	**0.03**	2.85	0.06	-7.87	**2.26E-03**	-5.02	**0.01**
	Unknown Benzene 1	40	9	9	0.64	0.22	0.06	1.00	-1.37	**0.01**	-1.30	**0.01**
	D-Limonene	40	9	9	-0.55	0.17	-0.63	0.63	0.44	1.00	-0.19	1.00
	Sabinene	40	9	9	0.12	0.20	0.21	0.21	-0.04	1.00	0.17	0.46
	Unknown Sesquiterpene 5	40	9	9	-0.03	**0.06**	-0.04	0.24	0.03	0.45	-0.01	1.00
	Unknown Sesquiterpene 7	40	9	9	-4.66E-04	0.96	-0.01	0.92	-0.01	1.00	-0.02	0.29
	Terpinolene	40	9	9	0.07	0.35	0.13	0.33	-0.01	1.00	0.12	0.44
	Unknown Monoterpene 1	40	9	9	-0.02	0.20	-0.02	0.83	0.02	0.88	0.00	1.00
	Unknown Monoterpene 3	40	9	9	0.01	**0.03**	0.01	0.31	-0.01	**0.03**	-0.01	0.31
	Unknown Monoterpene 4	40	9	9	0.01	0.10	4.38E-03	0.68	-0.02	**0.01**	-0.02	**0.02**
	β-Ocimene-2	40	9	9	-0.02	0.13	-0.02	0.63	0.02	0.75	-9.29E-04	1.00

	3-Carene	40	9	9	-0.45	0.61	0.50	1.00	1.48	0.27	1.98	0.13
	Total	40	9	9	16.57	0.10	5.10	1.00	-29.51	**0.01**	-24.41	**0.03**
Phloem Volatile Resin	α-Pinene	23	8	10	6.23	**0.02**	3.74	0.16	-8.38	**0.02**	-4.65	0.12
	γ-Terpinene	23	8	10	-0.02	0.14	-0.01	0.91	0.04	0.26	0.03	0.53
	Bornyl acetate	23	8	10	0.06	0.45	-0.03	0.96	-0.15	0.26	-0.19	0.18
	Limonene	23	8	10	-1.44	**0.01**	-1.47	0.06	1.42	0.11	-0.05	1.00
	Sabinene	23	8	10	-1.29	**0.05**	-1.20	0.27	1.36	0.24	0.16	0.99
	Methyl thymyl ether	23	8	10	0.53	0.12	0.08	0.96	-0.95	**0.03**	-0.87	**0.02**
	Unknown Sesquiterpene 3	23	8	10	0.05	0.21	0.01	0.99	-0.08	0.33	-0.07	0.50
	Unknown Sesquiterpene 4	23	8	10	1.55	**0.01**	1.41	**0.05**	-1.66	0.06	-0.25	0.93
	Unknown Sesquiterpene 20	23	8	10	-0.56	**0.05**	-0.54	0.25	0.57	0.28	0.03	1.00
	Unknown Sesquiterpene 21	23	8	10	-1.40	**0.02**	-1.41	0.09	1.39	0.17	-0.02	1.00
	Unknown Sesquiterpene 22	23	8	10	-0.12	**0.02**	-0.12	0.09	0.12	0.15	-0.01	1.00
	Terpinolene-2	23	8	10	-0.64	0.07	-0.49	0.50	0.77	0.24	0.27	0.88
	3-Carene	23	8	10	-0.87	0.24	0.05	1.00	1.61	0.30	1.66	0.32
	Tricyclene	23	8	10	-0.01	0.62	-0.02	0.60	-4.14E-03	0.99	-0.02	0.54
	Total	23	8	10	2.25	0.61	-1.41	0.99	-5.18	0.74	-6.59	0.68

NSCs	Fructose Concentration (Needles)	15	6	9	0.01	0.88	0.05	0.97	0.01	1.00	0.06	0.97
	Glucose Concentration (Needles)	15	6	9	0.37	**0.03**	0.36	0.20	-0.38	0.21	-0.02	1.00
	Glucose and Fructose Concentration (Needles)	15	6	9	0.39	0.11	0.41	0.42	-0.37	0.49	0.03	1.00
	Starch Concentration (Needles)	15	6	9	-0.02	0.78	-0.02	1.00	0.02	1.00	3.54E-03	1.00
	Sucrose Concentration (Needles)	15	6	9	0.25	**0.06**	0.24	0.38	-0.27	0.32	-0.03	1.00
	Total NSC Concentration (Needles)	15	6	9	0.60	0.08	0.62	0.36	-0.59	0.41	0.03	1.00
	Glucose, Fructose, and Sucrose Concentration (Needles)	15	6	9	0.63	**0.04**	0.64	0.21	-0.62	0.27	0.03	1.00
	Fructose Concentration (Roots)	15	6	9	0.02	0.56	0.01	1.00	-0.04	0.91	-0.03	0.95
	Glucose Concentration (Roots)	15	6	9	0.31	0.07	0.46	0.12	-0.22	0.57	0.24	0.57
	Glucose and Fructose Concentration (Roots)	15	6	9	0.33	0.08	0.43	0.19	-0.25	0.52	0.18	0.80
	Starch Concentration (Roots)	15	6	9	-0.06	0.55	-0.01	1.00	0.09	0.84	0.09	0.90
	Sucrose Concentration (Roots)	15	6	9	0.18	0.59	0.70	0.37	-0.07	1.00	0.63	0.53
	Total NSC Concentration (Roots)	15	6	9	0.44	0.41	0.99	0.44	-0.15	0.99	0.84	0.63
	Glucose, Fructose, and Sucrose Concentration (Roots)	15	6	9	0.50	0.30	0.93	0.40	-0.21	0.97	0.73	0.64
	Fructose Concentration (Stem)	16	6	8	0.04	0.75	0.08	0.94	-4.39E-03	1.00	0.08	0.96
	Glucose Concentration (Stem)	16	6	8	1.51	**0.02**	1.97	**0.02**	-1.05	0.18	0.92	0.30
	Glucose and Fructose Concentration (Stem)	16	6	8	1.50	**0.01**	1.93	**0.01**	-1.05	0.10	0.88	0.21

	Starch Concentration (Stem)	16	6	8	0.03	0.53	0.01	0.99	-0.03	0.89	-0.02	0.97
	Sucrose Concentration (Stem)	16	6	8	0.52	0.16	0.56	0.53	-0.48	0.62	0.09	1.00
	Total NSC Concentration (Stem)	16	6	8	1.98	**0.01**	2.48	**0.03**	-1.57	0.15	0.91	0.56
	Glucose, Fructose, and Sucrose Concentration (Stem)	16	6	8	1.96	**0.01**	2.48	**0.03**	-1.53	0.16	0.95	0.51

Appendix table 3: Results of linear mixed effects models comparing drought and control treatments after accounting for species. Bolded values indicate significant differences at p-value ≤ 0.05.

		Drought - Control			
		PIAL		PIBA	
	name	estimate	p-value	estimate	p-value
Morphology	Aboveground Biomass : Belowground Biomass	0.53	0.73	-0.19	1.00
	Mean Branch Diameter	0.19	0.81	0.01	1.00
	Mean Branch Length	4.23	0.79	-4.59	0.97
	Branch Diameter : Stem Diameter	-0.02	0.97	-0.02	1.00
	Branch Diameter : Branch Length	0.00	1.00	0.01	1.00
	Canopy Area	318.92	1.00	130.41	1.00
	Fascicle Density	0.04	0.70	0.01	1.00
	Leaf Area : Sapwood Area	56.91	1.00	665.14	**0.04**
	LMA	-2.12E-03	0.47	-5.03E-04	1.00
	Needle Dry Biomass	0.47	0.95	0.30	1.00
	Root Dry Biomass	-1.24	0.81	1.35	0.92
	STAR	4.22	1.00	-9.98	0.99
	Stem Diameter : Stem Height	-2.82E-04	1.00	-3.01E-03	1.00
	Stem Diameter	0.94	0.46	1.21	0.68
	Stem Dry Biomass	1.18	0.26	0.66	0.91
	Stem height	29.75	0.09	13.00	0.96
	Leaf Area (Total)	16.89	0.99	71.78	0.55

Stomata	Guard Cell Area	1.40E-05	0.99	2.14E-04	**0.01**
	Row Density	0.36	0.87	-0.88	0.58
	Number of Rows	0.02	1.00	-0.01	1.00
	Aperture Area	2.27E-07	1.00	2.64E-05	0.84
	Aperture Length	-9.97E-04	0.50	8.91E-04	0.91
	Number of Stomata	0.31	0.34	-0.30	0.79
Xylem	Annual Ring Width	-0.01	1.00	0.02	0.99
	Earlywood Cell Wall Thickness	7.84E-06	1.00	5.70E-05	0.82
	Earlywood Lumen Area	4.61E-06	0.95	1.22E-05	0.65
	Earlywood Ring Width	-0.09	0.24	0.03	0.95
	Earlywood Tracheid Density	1.16E-04	0.97	-2.31E-04	0.89
	Earlywood : Latewood Ring Width	-0.86	0.11	0.14	0.99
	Potential Hydraulic Conductivity (Kp)	9.21E-09	0.86	1.68E-08	0.62
	Latewood Cell Wall Thickness	-1.47E-04	0.94	2.31E-04	0.91
	Latewood Lumen Area	5.80E-06	0.57	6.92E-06	0.60
	Latewood Ring Width	0.09	**0.03**	-0.01	1.00
	Latewood Tracheid Density	-3.41E-04	0.69	-5.97E-04	0.46
	Resin Duct Area	-8.10E-05	0.98	2.29E-04	0.82
	Resin Duct Density	-0.62	1.00	1.18	0.99

	Vessel Implosion Resistance (VIR)	-0.07	0.73	-0.02	1.00
Budburst	Days between Stage 1 and Stage 2	3.88	0.99	0.03	1.00
	Days between Stage 1 and Stage 3	3.38	1.00	-61.75	0.16
	Days between Stage 1 and Stage 4	-22.69	0.17	-25.15	0.33
	Days between Stage 1 and Stage 5	-20.00	0.97	-35.40	0.48
	Days between Stage 1 and Stage 6	0.17	1.00	-11.15	0.84
Physiology	Photosynthetic Rate (A)	-1.36	1.00	0.89	1.00
	Water Potential Difference (Midday - Predawn)	-0.06	1.00	0.02	1.00
	Midday Water Potential	-0.20	0.11	0.06	1.00
	Pre-Dawn Water Potential	-0.17	0.10	1.17E-03	1.00
	Leaf Temperature	-1.28	0.16	-0.73	0.69
	Stomatal Conductance (gs)	-2.99E-03	1.00	0.01	0.62
Base	Health status	-1.00	0.22	-0.17	1.00
	Volumetric Water Content (handheld sensor)	-19.70	**0.00**	-16.98	**0.00**
Whole Plant VOCs	β-Ocimene-2	0.02	0.40	-0.01	1.00
	Unknown Monoterpene 3	3.67E-03	1.00	-0.01	**0.01**
	Unknown Monoterpene 4	1.66E-03	1.00	-0.01	**0.02**
	Unknown Sesquiterpene 5	9.32E-04	1.00	-3.83E-03	1.00

Phloem Volatile Resin	Sabinene	-0.39	0.90	-0.11	1.00
	Unknown Sesquiterpene 20	0.33	0.55	0.02	1.00
	Unknown Sesquiterpene 3	0.05	0.68	-0.01	1.00
	Unknown Sesquiterpene 4	0.05	1.00	-0.01	1.00
NSCs	Fructose Concentration (Needles)	0.13	0.85	-0.25	0.19
	Glucose Concentration (Needles)	0.20	0.74	-0.31	0.25
	Glucose and Fructose Concentration (Needles)	0.33	0.71	-0.54	0.16
	Starch Concentration (Needles)	0.10	0.90	0.01	1.00
	Sucrose Concentration (Needles)	-0.08	0.98	-0.02	1.00
	Total NSC Concentration (Needles)	0.29	0.94	-0.53	0.49
	Glucose, Fructose, and Sucrose Concentration (Needles)	0.24	0.94	-0.56	0.25
	Fructose Concentration (Roots)	-0.05	0.95	-0.12	0.45
	Glucose Concentration (Roots)	-0.29	0.58	-0.02	1.00
	Glucose and Fructose Concentration (Roots)	-0.27	0.71	-0.15	0.92
	Starch Concentration (Roots)	-0.61	**2.22E-03**	-0.21	0.41
	Sucrose Concentration (Roots)	-0.30	0.97	0.02	1.00
	Total NSC Concentration (Roots)	-1.16	0.53	-0.36	0.98
	Glucose, Fructose, and Sucrose Concentration (Roots)	-0.57	0.91	-0.15	1.00
	Fructose Concentration (Stem)	-0.45	0.07	0.22	0.51
	Glucose Concentration (Stem)	-0.44	0.30	-0.03	1.00
	Glucose and Fructose Concentration (Stem)	-0.90	0.15	0.34	0.81
	Starch Concentration (Stem)	0.06	0.92	0.04	0.98

	Sucrose Concentration (Stem)	-0.14	1.00	0.61	0.61
	Total NSC Concentration (Stem)	-1.02	0.59	1.05	0.40
	Glucose, Fructose, and Sucrose Concentration (Stem)	-1.06	0.55	1.04	0.41